CHAPTER V

RESULT AND DISCUSSION

The results of the simulations are presented in 4 subsections, referring to the ion influence on the solvent's structure, the solvation of the cation, of the anion and the combination of these effects.

The following notations will be used to represent the atoms of hydroxylamine and water : $O_{(w)}$, $H_{(w)}$ and $CoM_{(w)}$ for oxygen atom, hydrogen atom and center-of-mass of water, respectively and $O_{(h)}$, $N_{(h)}$, $H_{O(h)}$, $H_{N(h)}$ and $CoM_{(h)}$ for oxygen atom, nitrogen atom, hydrogen atom connected to oxygen, hydrogen atoms connected to nitrogen and center-of-mass of hydroxylamine, respectively.

Solvent Structure

In order to investigate structure changes of hydroxylamine - water mixtures, caused by the presence of LiCl, the $H_{N(h)}$ -$O_{(w)}$ and $H_{O(h)}$ - $O_{(h)}$ RDFs for both cases, with and without LiCl (taken from reference 32), have been compared in Figure 5.1 and 5.2, respectively. Only some minor changes, induced by the ions, have been found. Hydrogen bonding framework in the solvent is exhibited by the presence of the shoulder at 2.2 Å and 2.0 Å of the $H_{N(h)}$ -$O_{(w)}$ and $H_{O(h)}$ - $O_{(h)}$ RDFs, respectively. These shoulders for the LiCl solution (Figure 5.1 b and 5.2 b) is less pronounce than these of the mixed solvents (Figure 5.1 a and 5.2 a). This indicates the less hydrogen bond framework in the LiCl solutions.

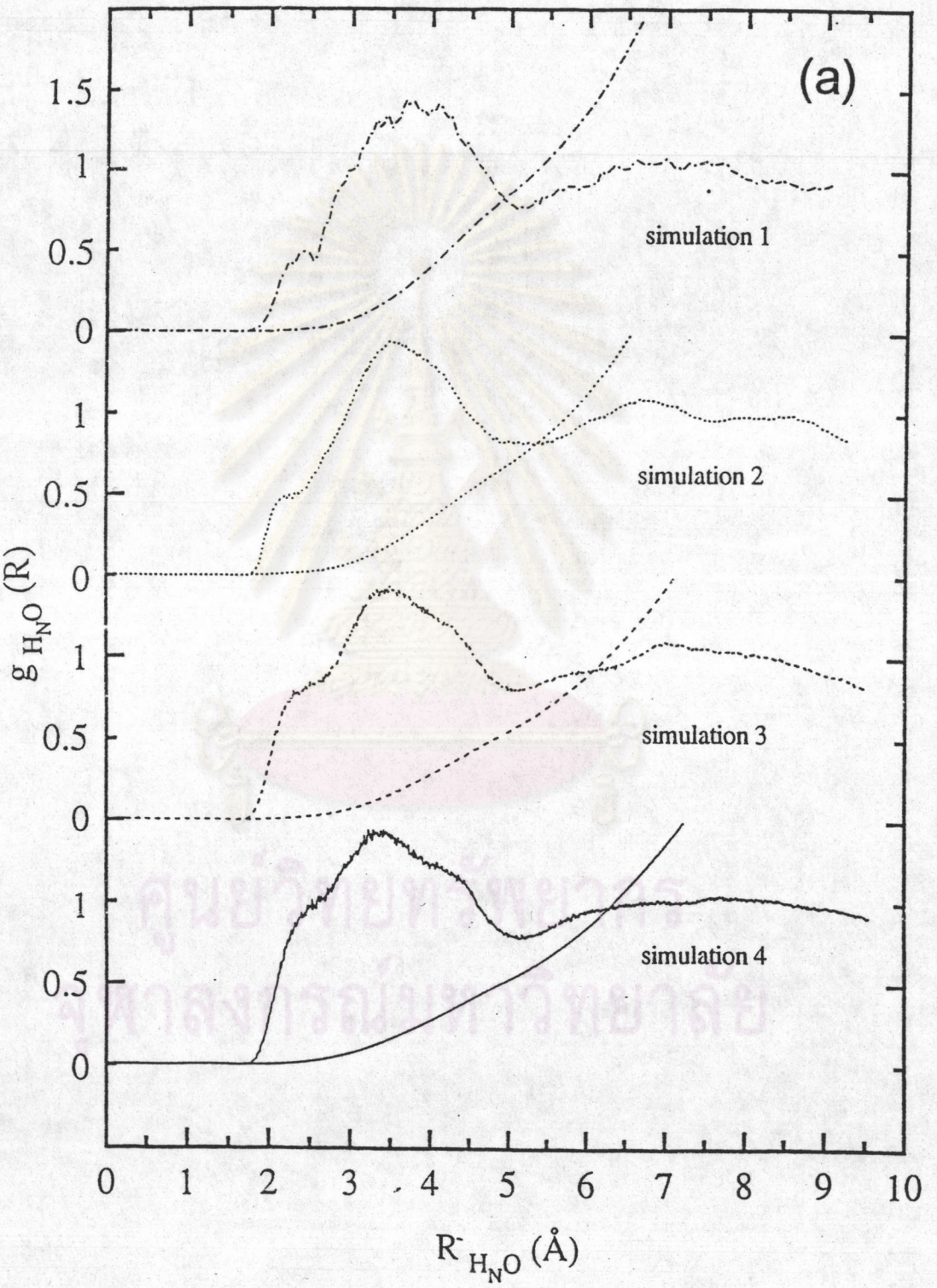
(a)
simulation 1
simulation 2
simulation 3
simulation 4
$g_{H_NO}(R)$
R_{H_NO} (Å)
0
0.5
1
1.5
0
1
2
3
4
5
6
7
8
9
10

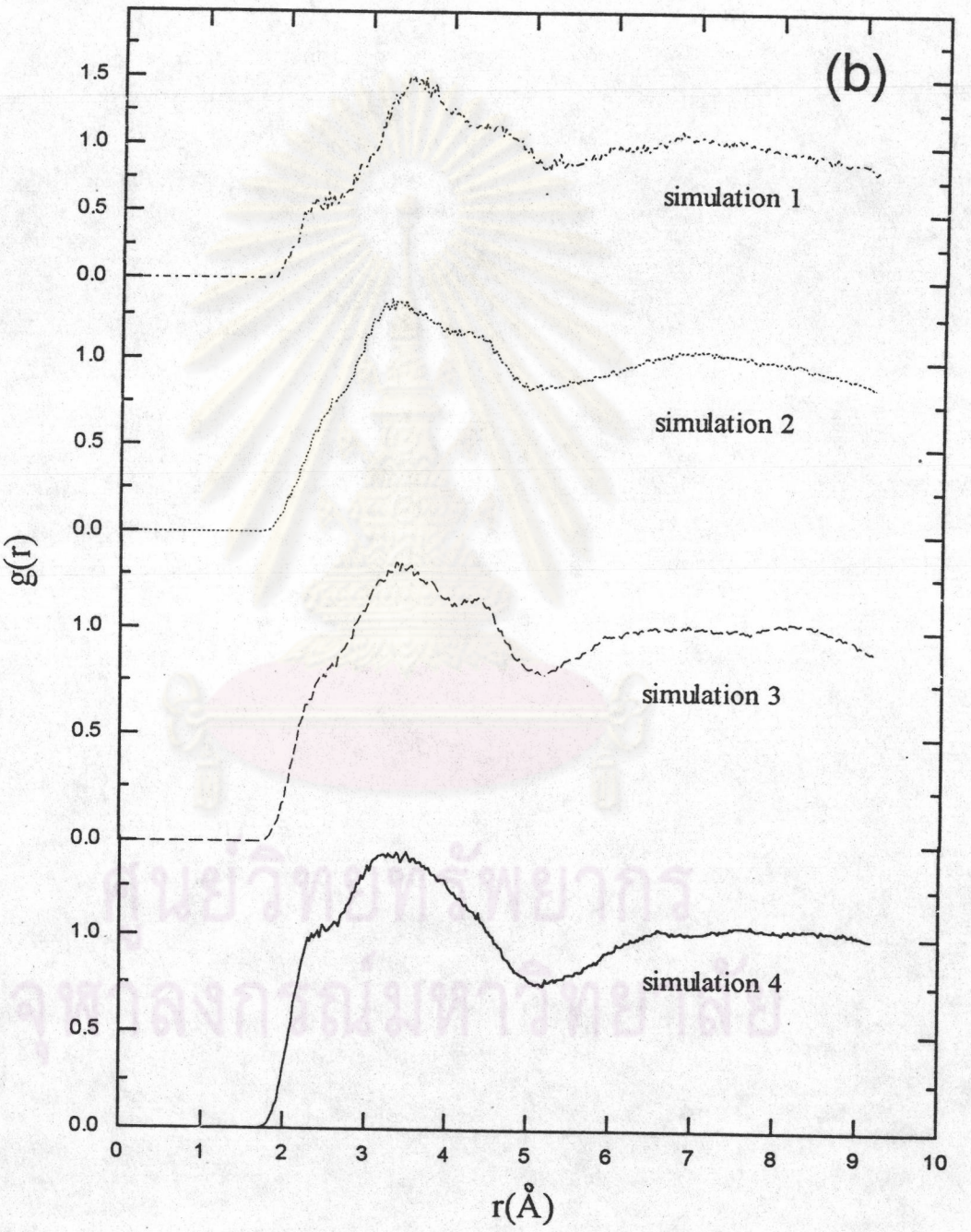

Figure 5.1 $H_{N(h)}$ - $O_{(w)}$ radial distribution functions for (a) without LiCl and (b) with LiCl.

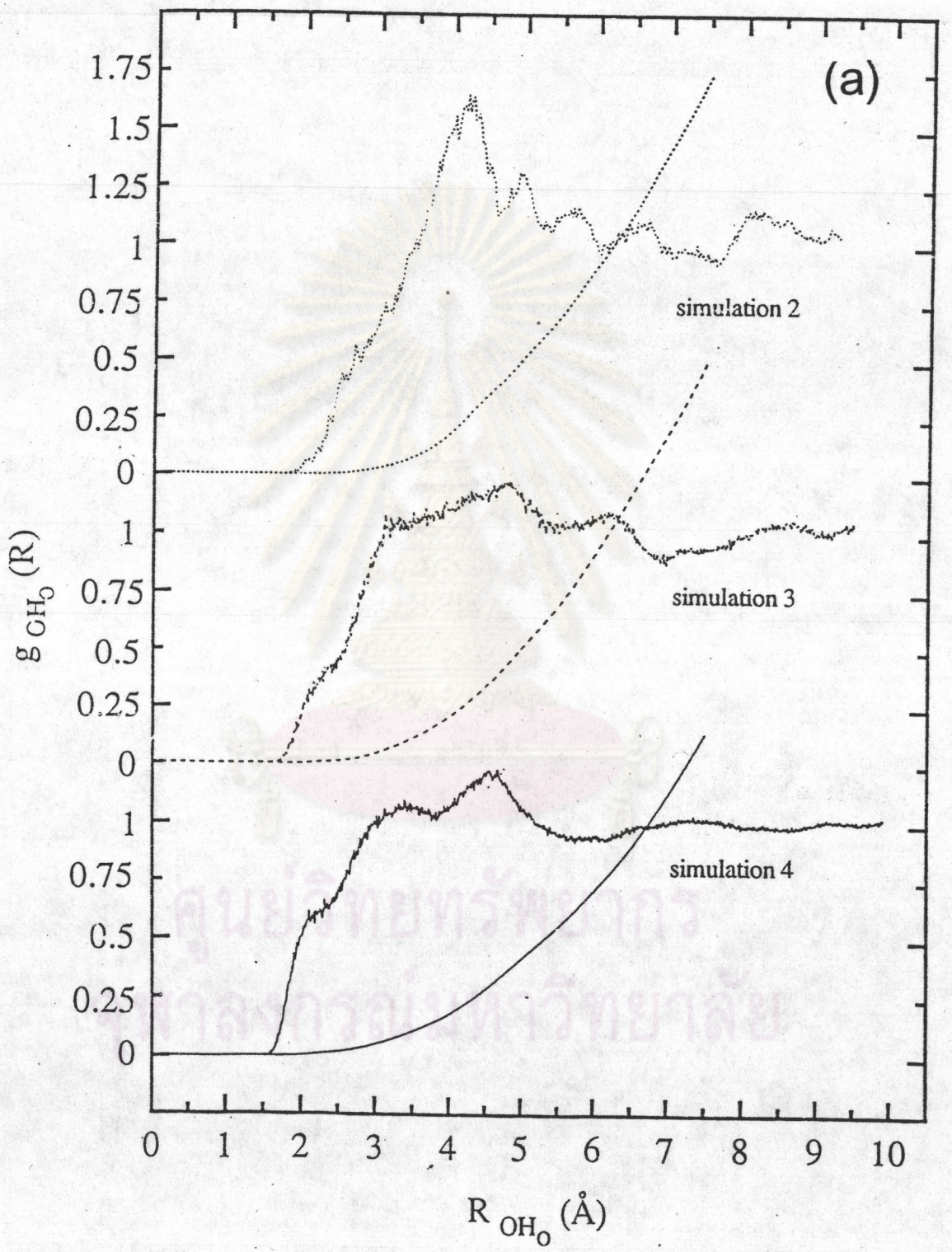
(a)
simulation 2
simulation 3
simulation 4
$g_{CH_O}(R)$
R_{OH_O} (Å)
1.75
1.5
1.25
1
0.75
0.5
0.25
0
0 1 2 3 4 5 6 7 8 9 10

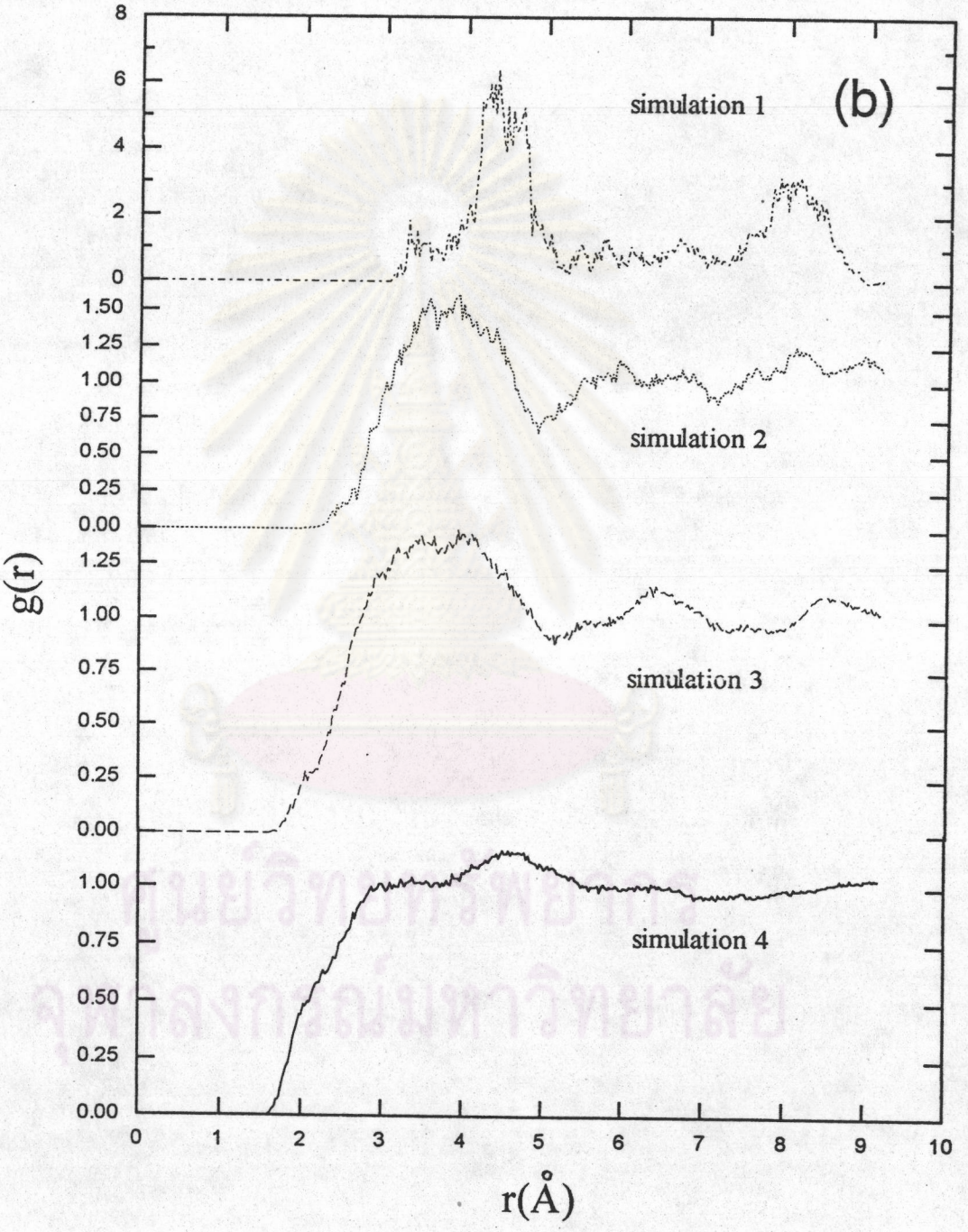

Figure 5.2 $H_{O(h)}$ - $O_{(h)}$ radial distribution functions for (a) without LiCl and (b) with LiCl.

All other RDFs are nearly identical to those reported for the solvent mixtures themselves (32).

Li^+ Solvation

The RDFs for water and hydroxylamine coordinated to Li^+ for each composition are different from each other. This data indicate the changes of solvent structure around the ion from one to another mixture.

5.1) 4.5% weight NH_2OH

When only 4.5% NH_2OH are contained in the solvent, only water molecules are in the first solvation shell of Li^+ . The RDFs are shown in Figure 5.3, together with their running integration, the characteristic data of these are collected in Table 5.1. Li^+ is coordinated to 6 water molecules and the analysis of the history files shows that over 98% (Figure 5.4) of the configurations correspond to $[Li(H_2O)_6]^+$ at 2.2 Å (Figure 5.3 a). Figure 5.3 a , b and c , Li - hydroxylamine RDFs, show that no hydroxylamine is observed in the first shell. The $Li\text{-}O_{(w)}$ RDF proves dipole-oriented arrangement of the six ligands. A second hydration shell can be identified clearly around 4.3 Å, containing further 19 water molecules.

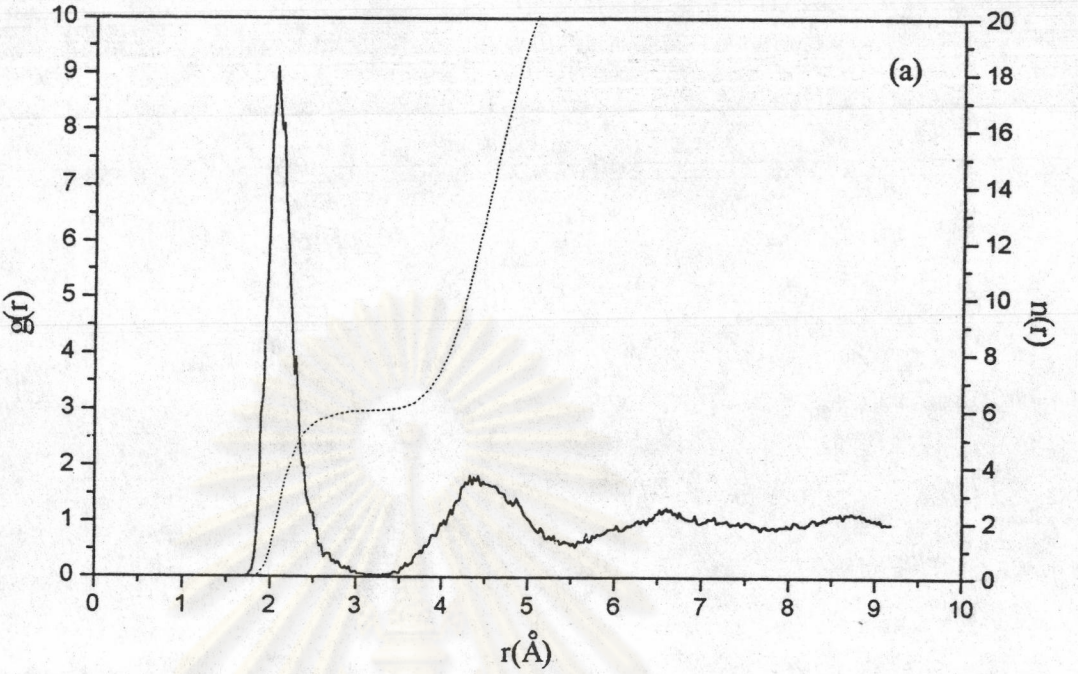
(a)
g(r)
n(r)
r(Å)
0
1
2
3
4
5
6
7
8
9
10
0
2
4
6
8
10
12
14
16
18
20

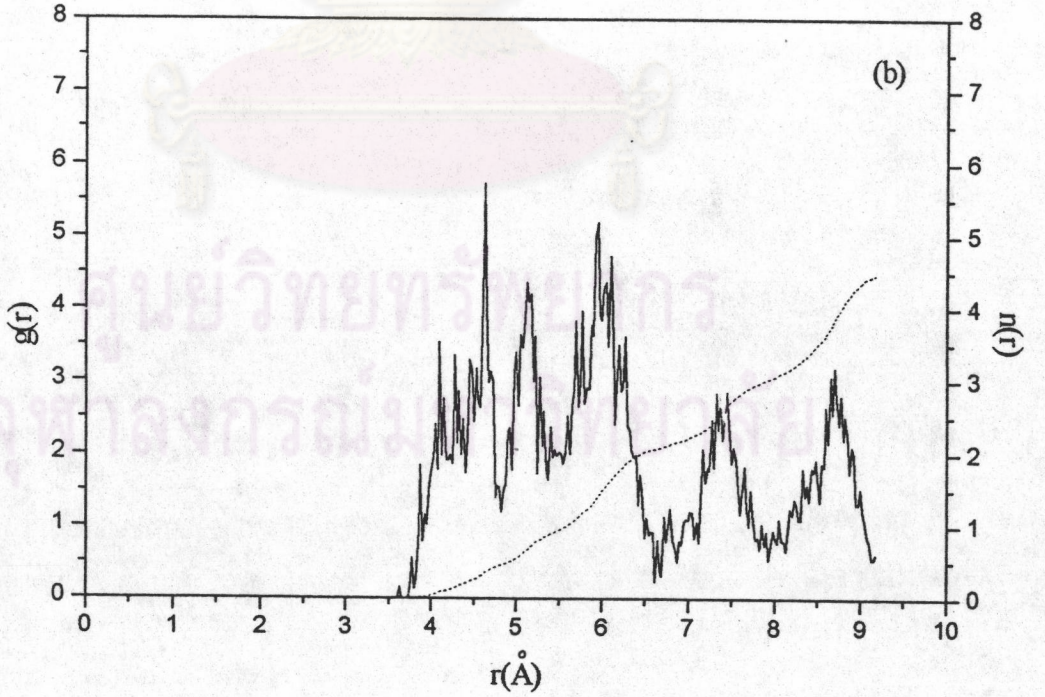
(b)
g(r)
n(r)
r(Å)
0
1
2
3
4
5
6
7
8
9
10
0
1
2
3
4
5
6
7
8

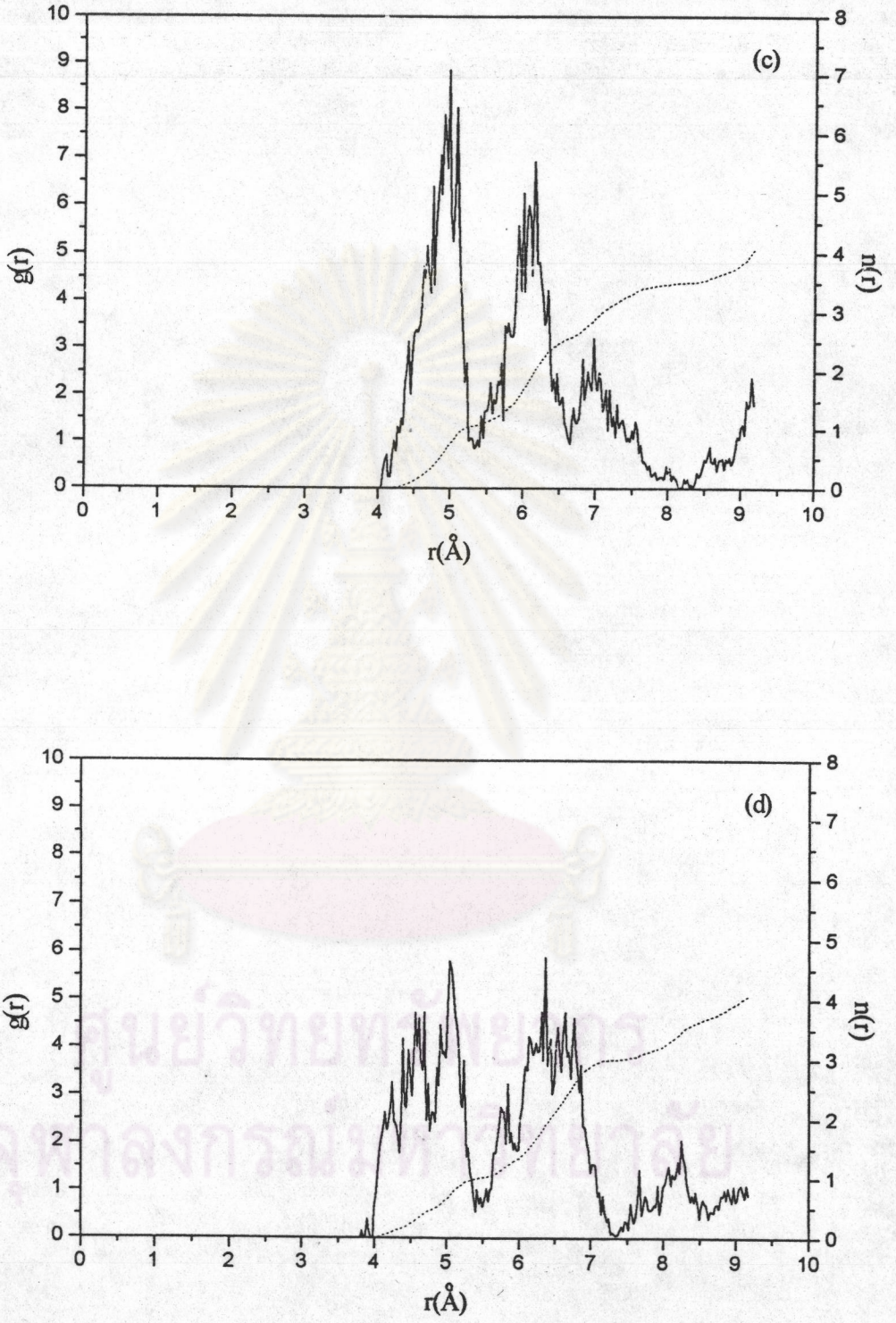

Figure 5.3 Radial distribution functions and running integration numbers for Li^+ in 4.5% by weight NH_2OH ; (a) $Li\text{-}O_{(w)}$, (b) $Li\text{-}O_{(h)}$, (c) $Li\text{-}N_{(h)}$, (d) $Li\text{-}CoM_{(h)}$.

Table 5.1 Characteristic values of radial distribution functions within the first coordination sphere of Li^+ with 4.5% by weight NH_2OH, r_{max} and r_{min} denote the first maximum and minimum of the RDF, and n is the integration up to r_{min}.

RDF	r_{max}	r_{min}	n
$Li\text{-}O_{(w)}$	2.075	3.300	6.0
$Li\text{-}H_{(w)}$	2.750	3.600	12.0
$Li\text{-}O_{(h)}$	-	-	-
$Li\text{-}N_{(h)}$	-	-	-
$Li\text{-}CoM_{(h)}$	-	-	-

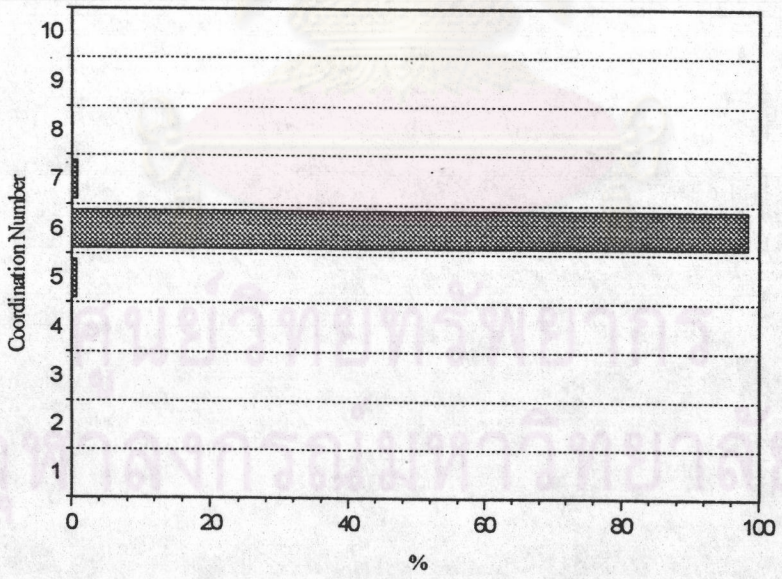

Figure 5.4 Coordination number distribution for Li - $CoM_{(w)}$ in 4.5% by weight NH_2OH.

5.2) 25% weight NH_2OH

With NH_2OH concentration increasing to 25%, see Figure 5.5 and Table 5.2, the average number of water ligands in the first coordination shell decreases to 4 (Figure 5.5 a), and at the same time hydroxylamine molecules enter this shell, in average coordinated to the same extent via O and N of NH_2OH. This average composition $[Li(H_2O)_4(NH_2OH)_2]^+$ results, according to the coordination number distribution analysis, Figure 5.6, mainly from 2 species, namely $[Li(H_2O)_5(NH_2OH)]^+$ and $[Li(H_2O)_3(NH_2OH)_3]^+$. Only about 6% of the solvated ions are really present as $[Li(H_2O)_4(NH_2OH)_2]^+$. A second solvation shell can be recognized as well, containing in average 14 water and 3-4 hydroxylamine molecules.

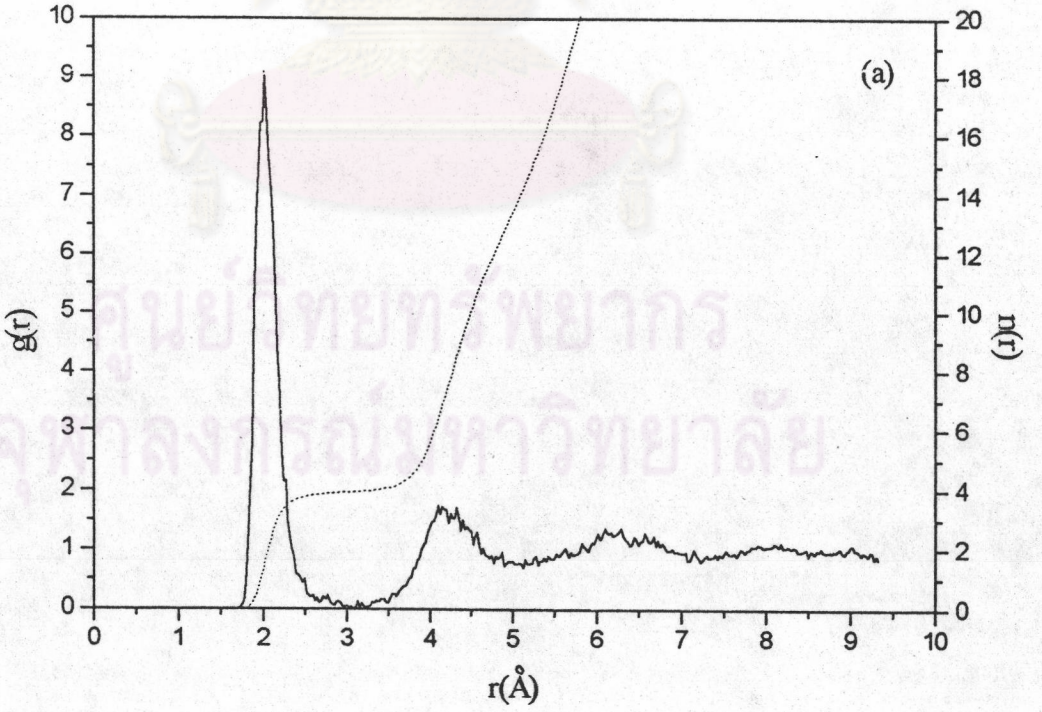

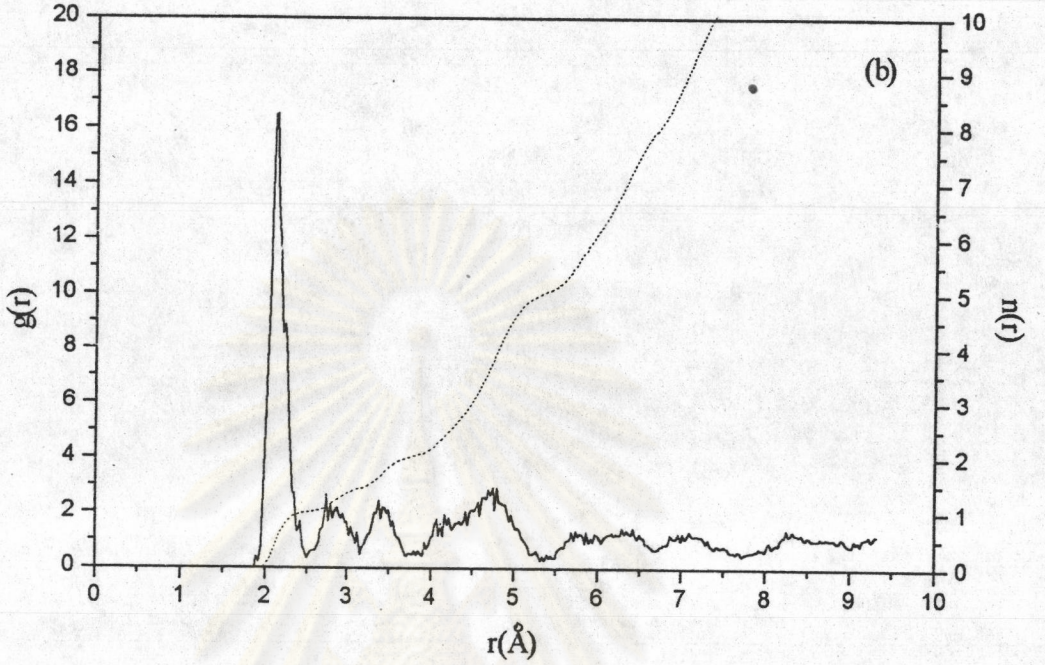

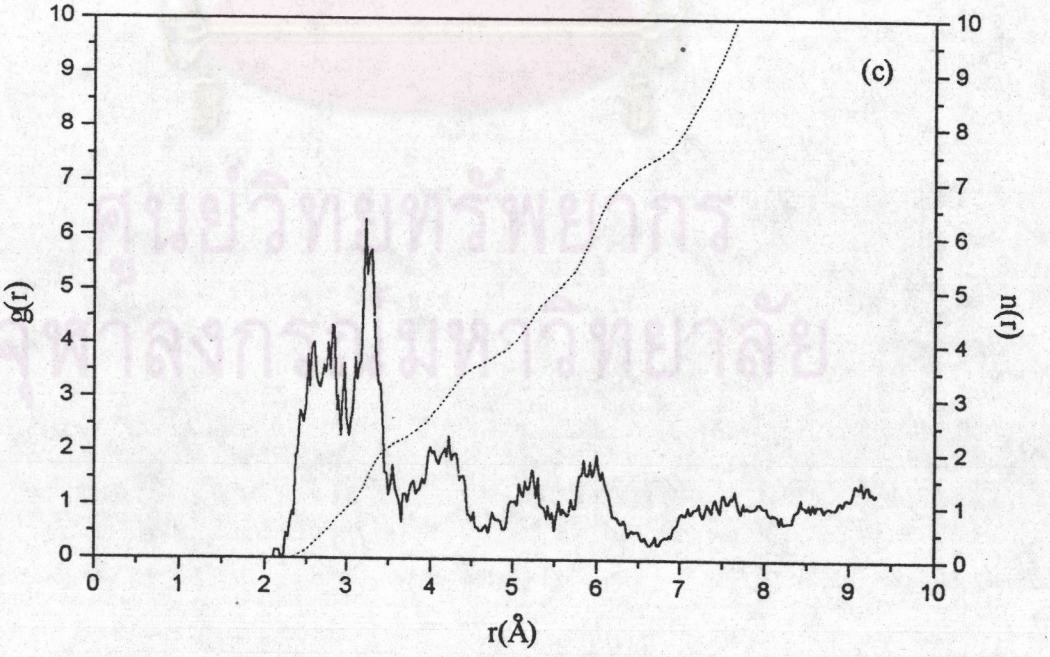

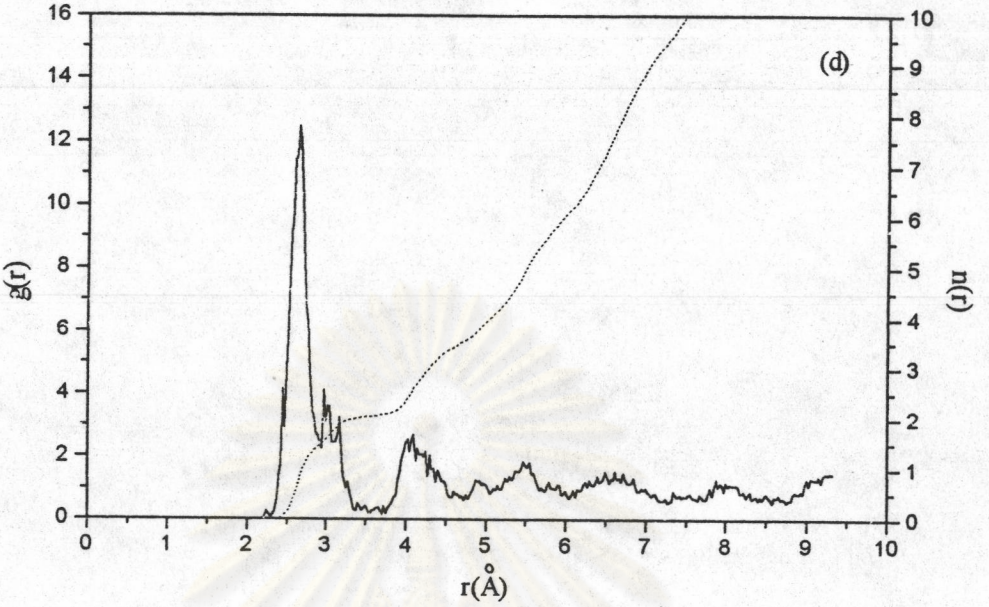

Figure 5.5 Radial distribution functions and running integration numbers for Li^+ in 25% by weight NH_2OH ; (a) $Li\text{-}O_{(w)}$, (b) $Li\text{-}O_{(h)}$, (c) $Li\text{-}N_{(h)}$, (d) $Li\text{-}CoM_{(h)}$.

Table 5.2 Characteristic values of radial distribution functions within the first coordination sphere of Li^+ with 25% by weight NH_2OH, r_{max} and r_{min} denote the first maximum and minimum of the RDF, and n is the integration up to r_{min}.

RDF	r_{max}	r_{min}	n
$Li\text{-}O_{(w)}$	2.025	3.075	4.0
$Li\text{-}H_{(w)}$	2.700	3.500	8.0
$Li\text{-}O_{(h)}$	2.125	2.500	1.0
$Li\text{-}N_{(h)}$	2.825	3.500	2.0
$Li\text{-}CoM_{(h)}$	2.650	3.375	2.0

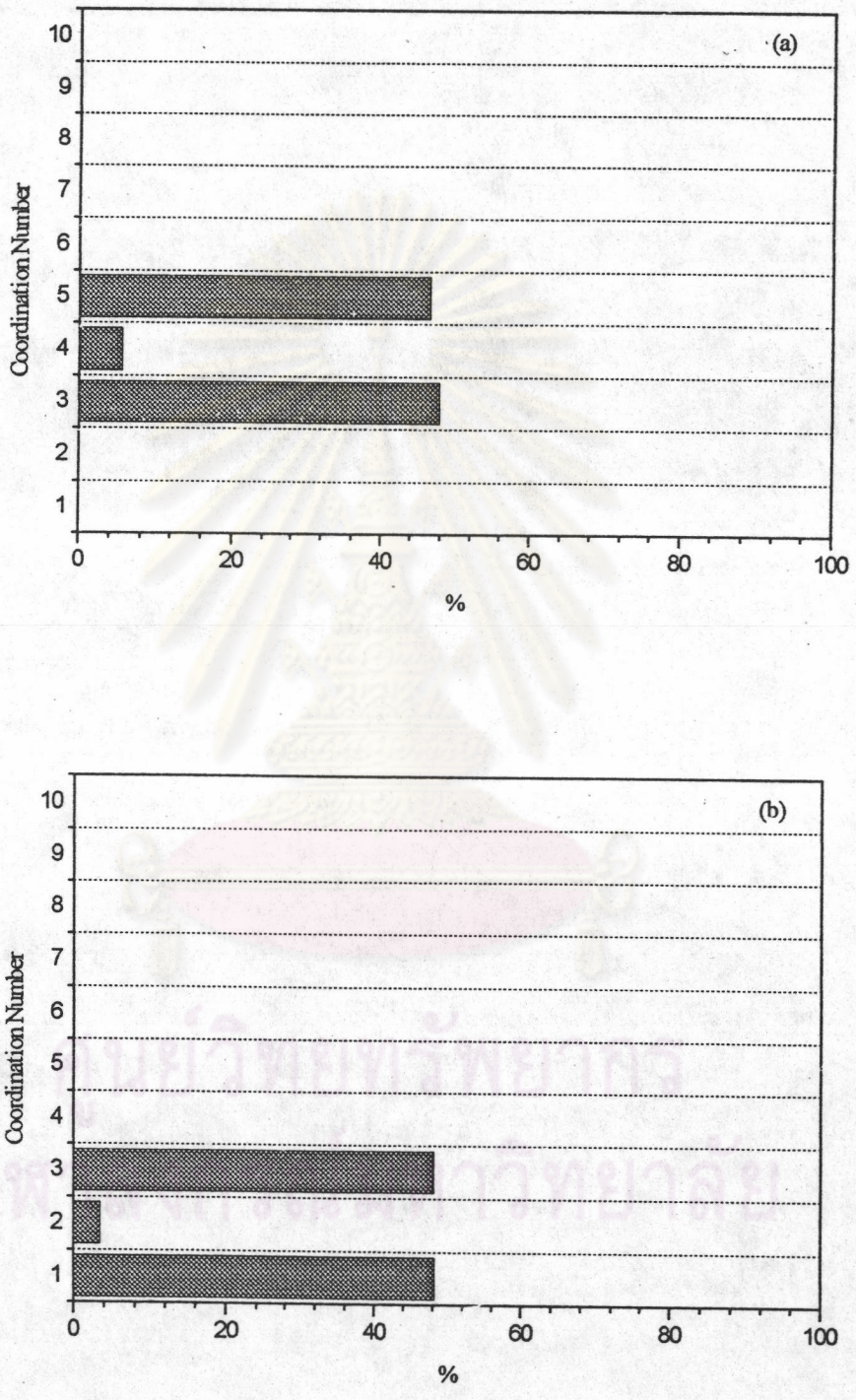

Figure 5.6 Coordination number distribution for (a) Li-$CoM_{(w)}$ and (b) Li-$CoM_{(w)}$ in 25% by weight NH_2OH.

5.3) 50% weight NH_2OH

When 50% of the ligand molecules are NH_2OH (Figure 5.7 and Table 5.3), the average composition of solvated Li^+ is given as $[Li(H_2O)_{2.5}(NH_2OH)_3]^+$. Coordination number of 2.5 water molecules around Li^+ is averaged from 43% of 2 and 57% of 3 (Figure 5.8), which the number of 3 NH_2OH ligands in the first shell is almost exclusive (97%). The $Li\text{-}O_{(h)}$ and $Li\text{-}N_{(h)}$ RDFs show that all 3 NH_2OH ligands are coordinated via oxygen under these circumstances. A second solvation shell is less discernible in this environment and has to be assumed to extend to more than 6 Å in diameter and thus appears not really well separated from the surrounding bulk.

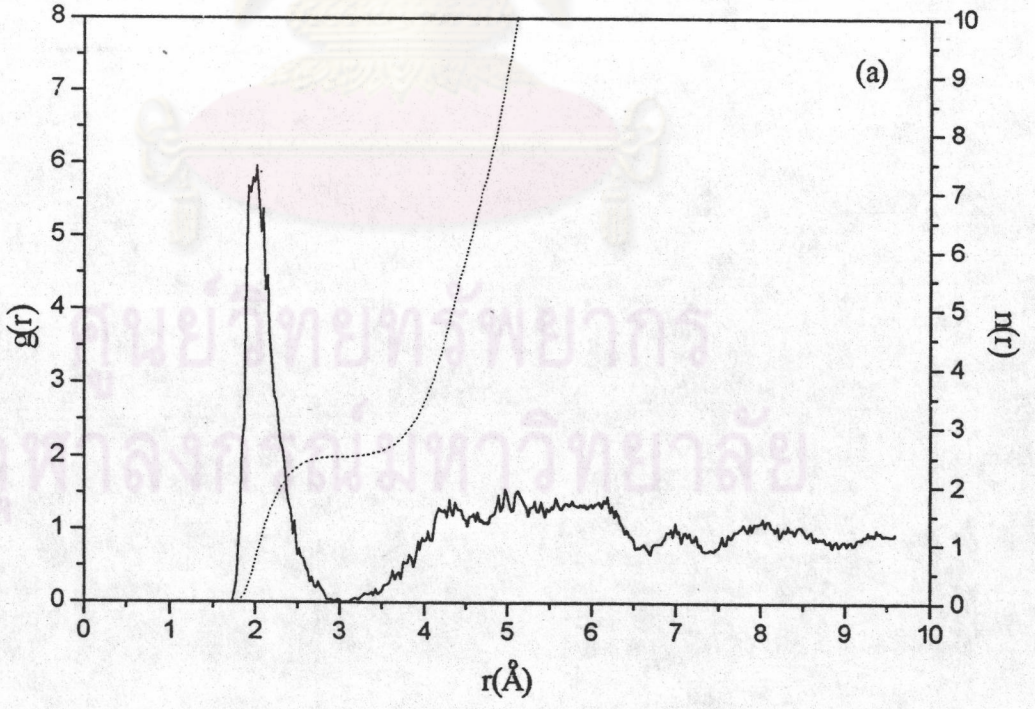

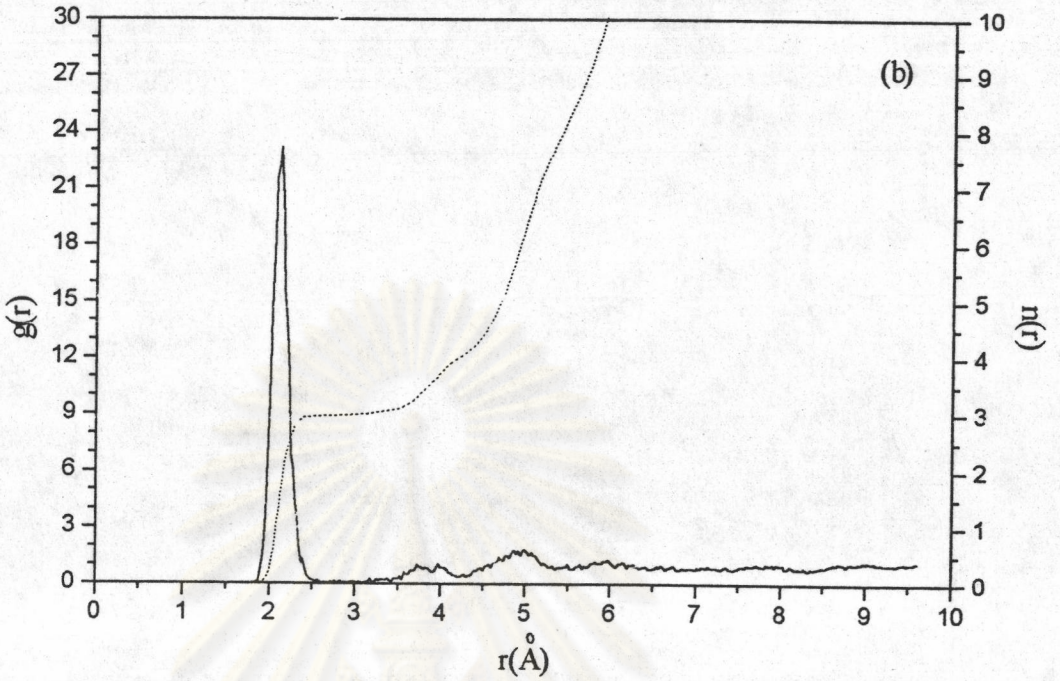
(b)
g(r)
n(r)
r(Å)

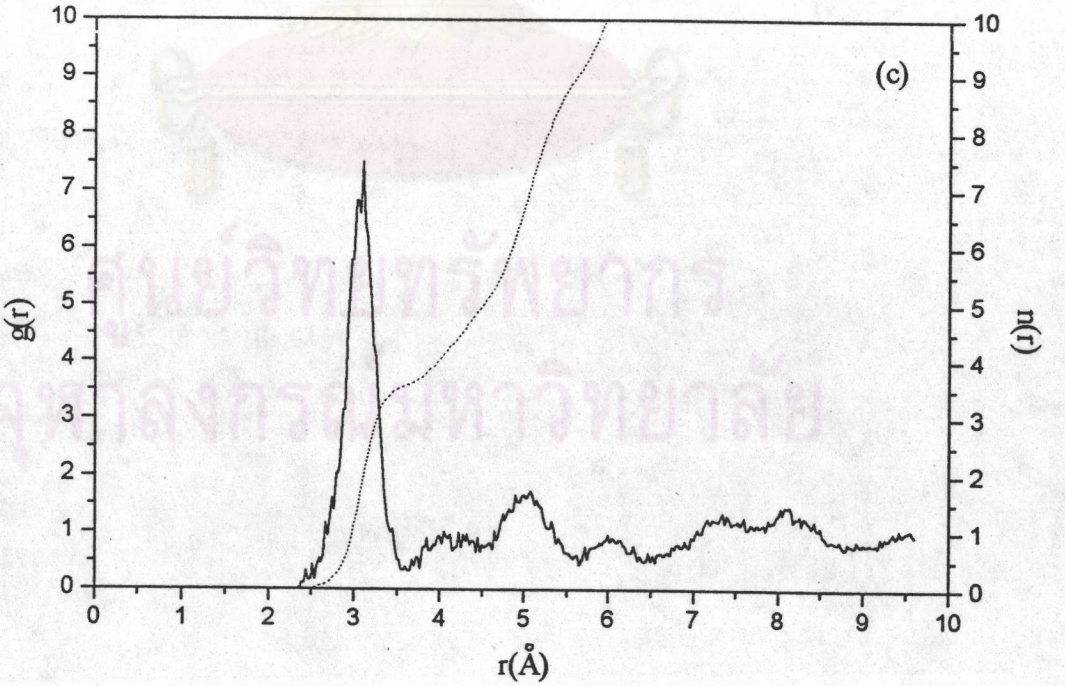
(c)
g(r)
n(r)
r(Å)

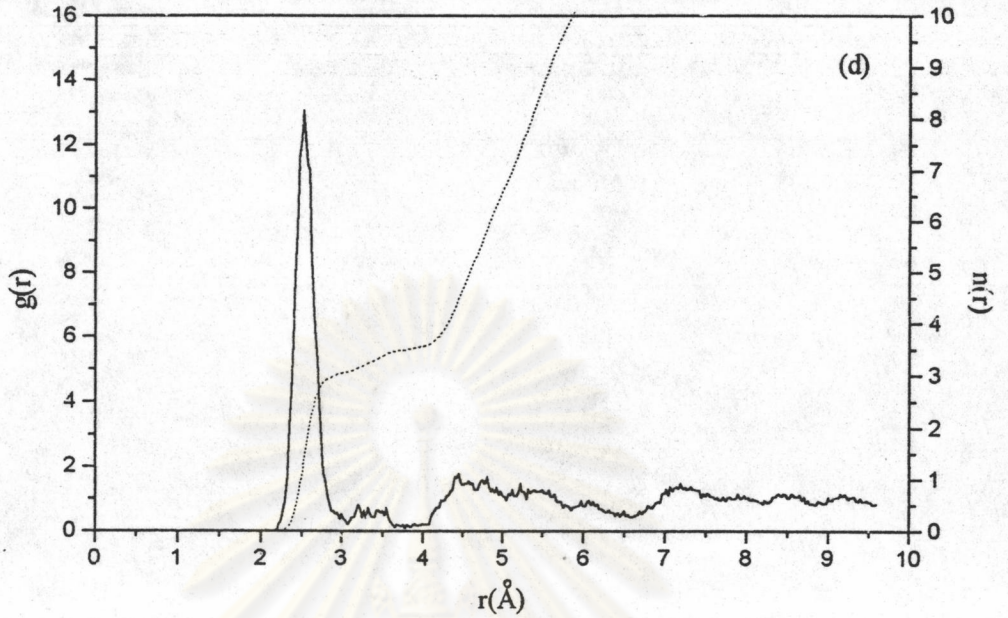

Figure 5.7 Radial distribution functions and running integration numbers for Li^+ in 50% by weight NH_2OH ; (a) $Li\text{-}O_{(w)}$, (b) $Li\text{-}O_{(h)}$, (c) $Li\text{-}N_{(h)}$, (d) $Li\text{-}CoM_{(h)}$.

Table 5.3 Characteristic values of radial distribution functions within the first coordination sphere of Li^+ with 50% by weight NH_2OH, r_{max} and r_{min} denote the first maximum and minimum of the RDF, and n is the integration up to r_{min}.

RDF	r_{max}	r_{min}	n
$Li\text{-}O_{(w)}$	2.025	3.025	2.5
$Li\text{-}H_{(w)}$	2.650	3.375	5.0
$Li\text{-}O_{(h)}$	2.125	2.700	3.0
$Li\text{-}N_{(h)}$	2.100	3.550	3.5
$Li\text{-}CoM_{(h)}$	2.525	3.075	3.0

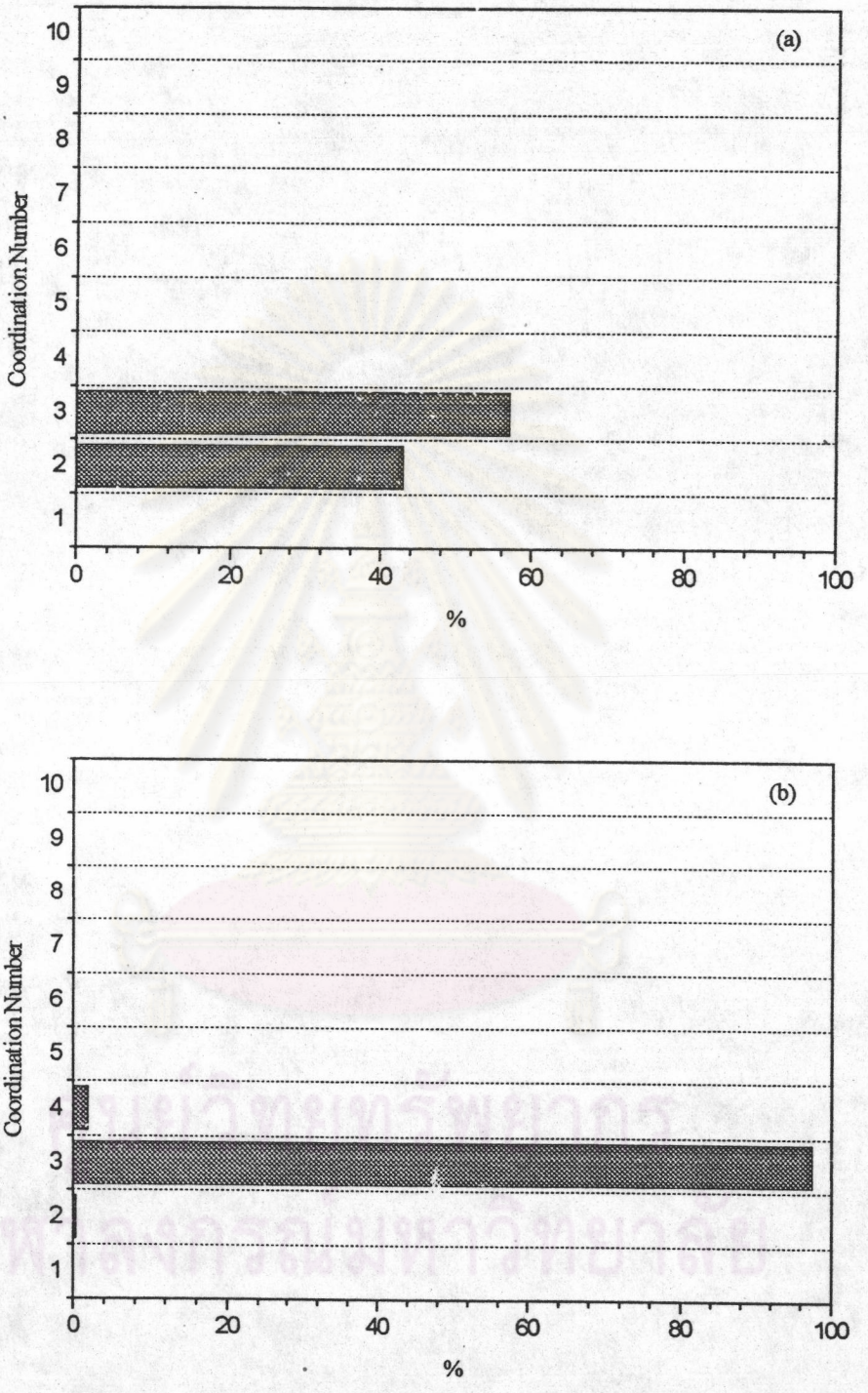

Figure 5.8 Coordination number distribution for (a) Li-$CoM_{(w)}$ and (b) Li-$CoM_{(h)}$ in 50% by weight NH_2OH.

5.4) 75% weight NH_2OH

Upon further increase of the hydroxylamine content to 75% of the solvent molecules, shown in Figure 5.9 and Table 5.4, the average species formula becomes $[Li(H_2O)_{1.5}(NH_2OH)_5]^+$. Analysis of the configurations in the solution reveals that water coordination numbers 1 and 2 are evenly distributed (Figure 5.10 a), combined with either 6 or 4 hydroxylamine ligands (Figure 5.10 b), respectively. Coordination of NH_2OH via oxygen dominates, but compared to the 50% solution N coordination also occurs to a considerable extent. The increased $Li\text{-}O_{(w)}$ distance reflects the general increase of the first solvation shell's diameter and the difficulty to place water ligands at optimal positions in the hydroxylamine-dominated surrounding. In order to reach the coordination number of 8 NH_2OH molecules found for Li^+ in pure hydroxylamine (29), the water content has to decrease apparently much more, and formation of species as $[Li(H_2O)(NH_2OH)_{6\text{-}7}]^+$ is likely at hydroxylamine concentrations above 80%. A discrete second solvation shell cannot be defined according to the RDFs obtained for the all mixtures.

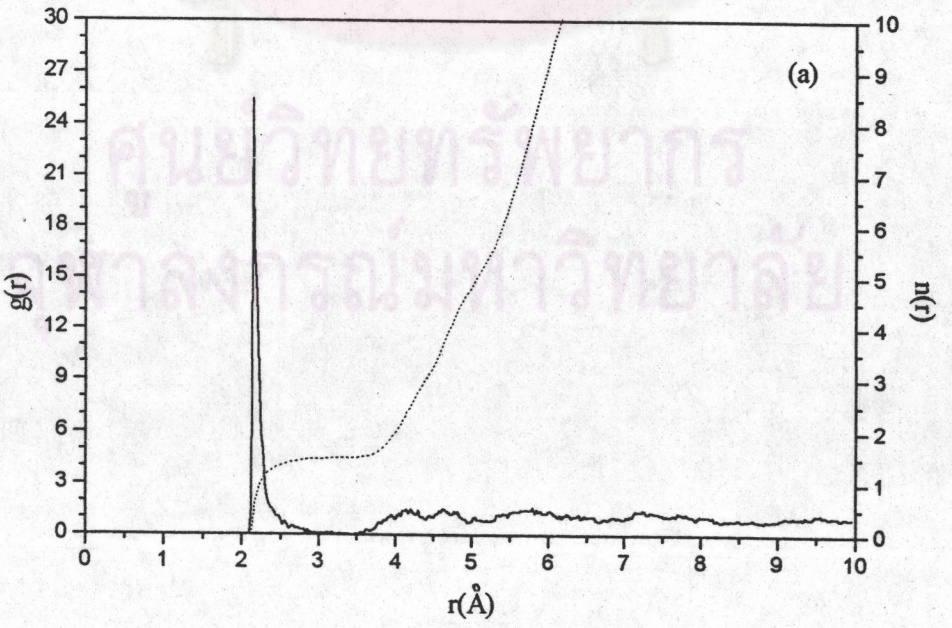

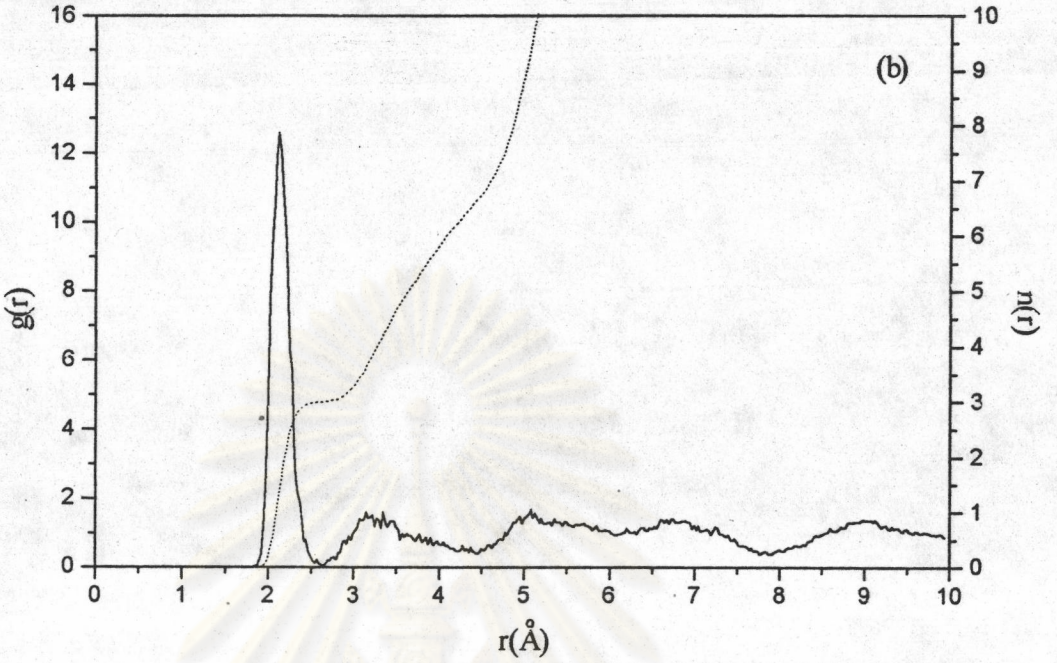
(b)
g(r)
n(r)
r(Å)
0
2
4
6
8
10
12
14
16
0
1
2
3
4
5
6
7
8
9
10

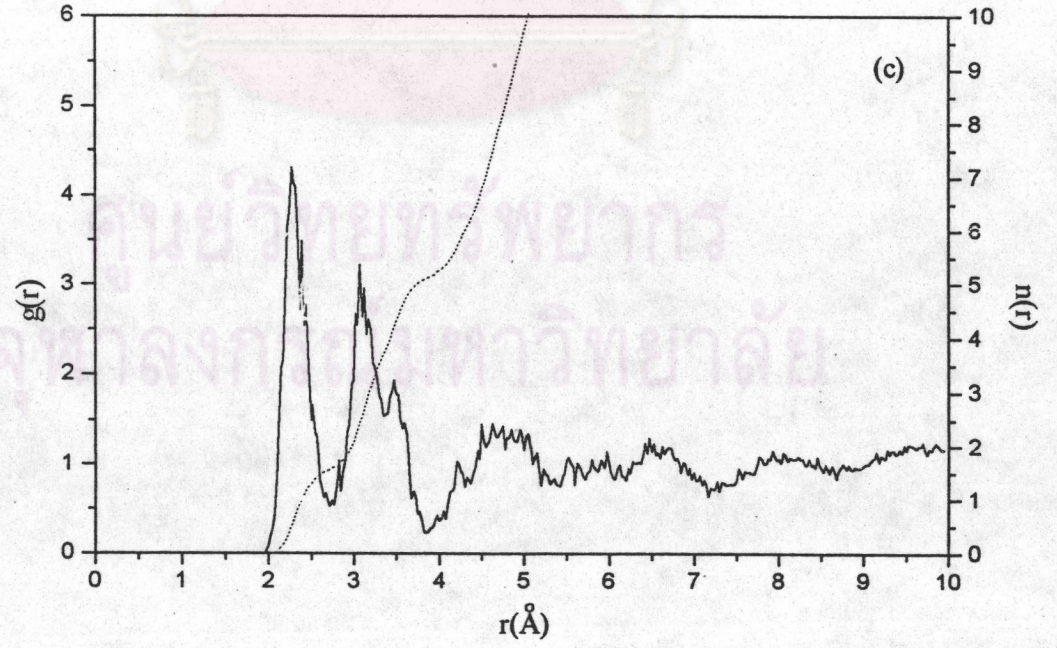
(c)
g(r)
n(r)
r(Å)
0
1
2
3
4
5
6
0
1
2
3
4
5
6
7
8
9
10

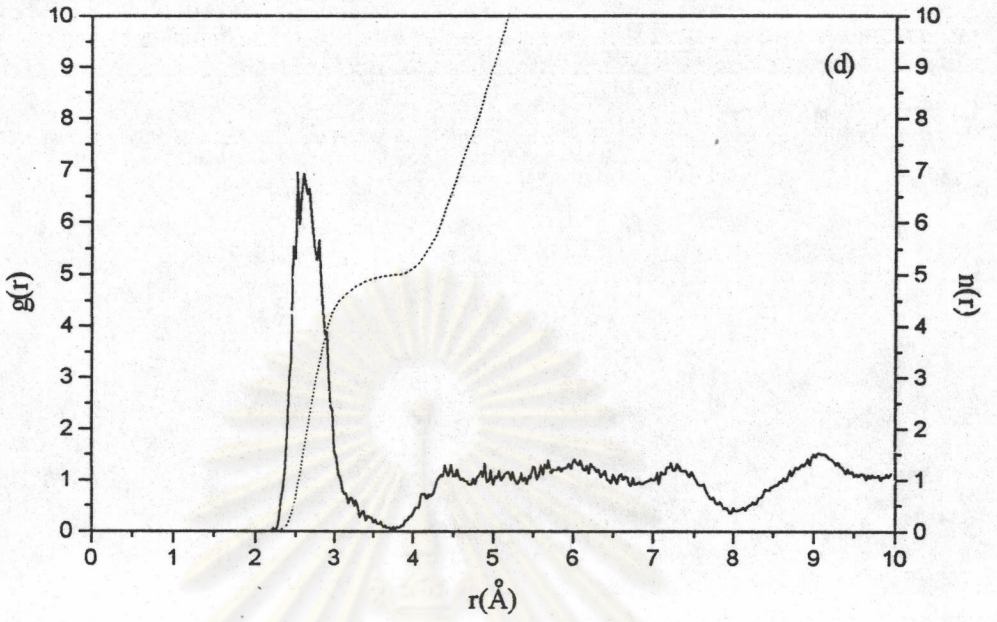

Figure 5.9 Radial distribution functions and running integration numbers for Li^+ in 75% by weight NH_2OH ; (a) $Li\text{-}O_{(w)}$, (b) $Li\text{-}O_{(h)}$, (c) $Li\text{-}N_{(h)}$, (d) $Li\text{-}CoM_{(h)}$.

Table 5.4 Characteristic values of radial distribution functions within the first coordination sphere of Li^+ with 75% by weight NH_2OH, r_{max} and r_{min} denote the first maximum and minimum of the RDF, and n is the integration up to r_{min}.

RDF	r_{max}	r_{min}	n
$Li\text{-}O_{(w)}$	2.150	3.300	1.5
$Li\text{-}H_{(w)}$	2.825	3.425	3.0
$Li\text{-}O_{(h)}$	2.125	2.650	3.0
$Li\text{-}N_{(h)}$	2.275	2.725	1.5
$Li\text{-}CoM_{(h)}$	2.525	3.725	5.0

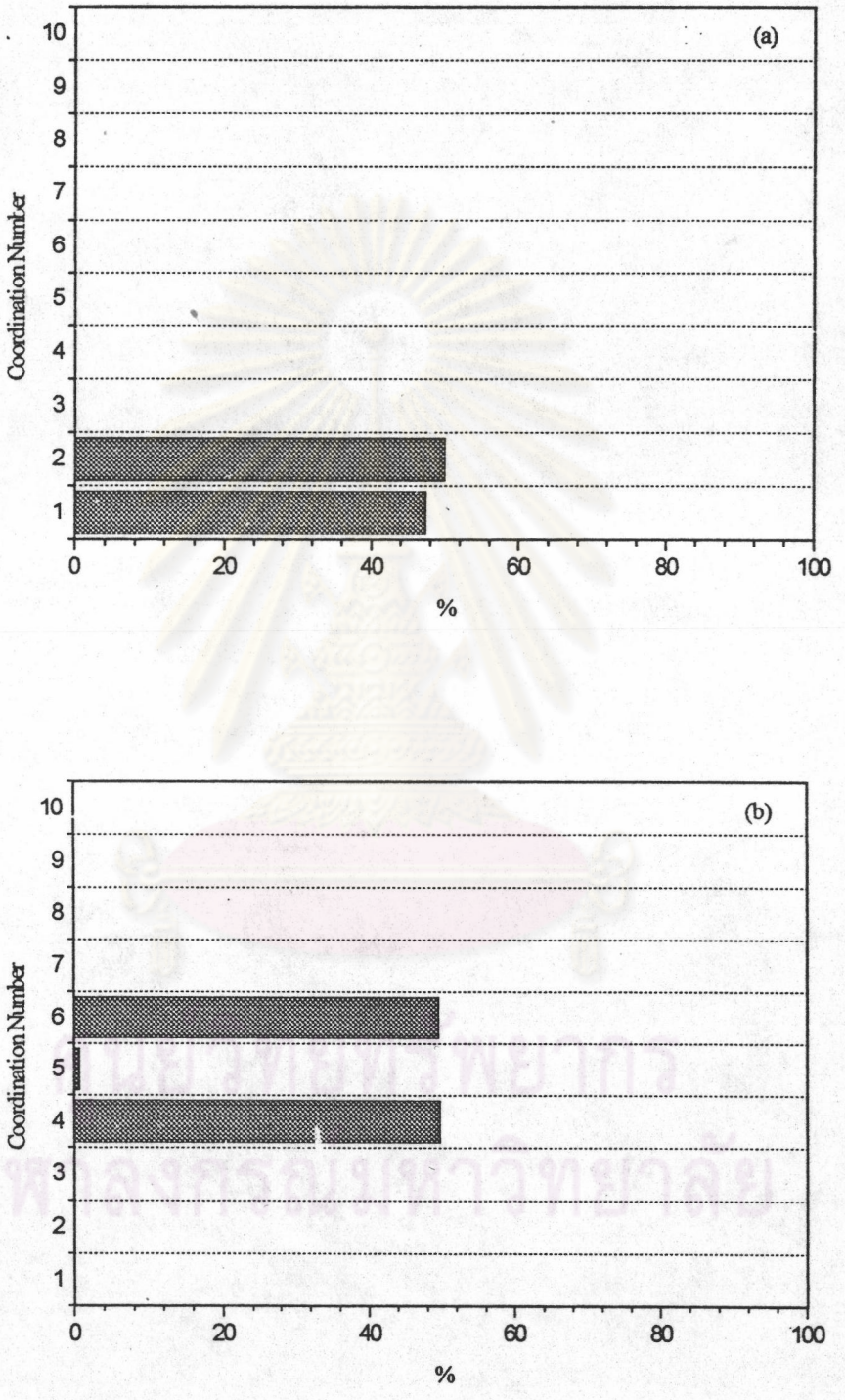

Figure 5.10 Coordination number distribution for (a) Li-$CoM_{(w)}$ and (b) Li-$CoM_{(h)}$ in 75% by weight NH_2OH.

Summarizing the results of the four simulations, 6 seems to remain the favoured coordination number of Li^+ over the whole investigated concentration range. Preference for binding to NH_2OH is observed up to high NH_2OH concentrations, oxygen being the favoured coordination site. The resulting average compositions of the solvated species $[Li(H_2O)_n(NH_2OH)_m]^+$ appear to be compromise arrangements, therefore, making use of the different coordination sites of NH_2OH and the possibility to fit water molecules into the space between the preferentially bound hydroxylamine ligands. The 50% solution apparently offers good conditions for this purpose so that all NH_2OH ligands can be bound via the O-coordination site preferred by the Li^+, but does not seem to offer "ideal" water coordination conditions then. Water orientation does not change from the dipole-oriented one throughout the series; once water becomes a first shell ligand, this seems to be by far the most favourable orientation so that compromises are imposed rather on the orientation of NH_2OH ligands.

Cl^- Solvation

The characteristics of the RDFs and those most relevant for the discussion of structural details are shown under each subsection.

5.5) 4.5% weight NH_2OH

The RDFs of these composition are shown in Figure 5.11 and Table 5.5. The presence of a small amount NH_2OH in the solution does not change the composition of the anion's solvation shell familiar from simulations of Cl^- in pure water. The average composition $[Cl(H_2O)_8]^-$ results from a normal distribution of coordination numbers

between 6 and 10 (Figure 5.12), and all water molecules are connected to the central ion via H-bonds, according to the Cl-$H_{(w)}$ RDF.

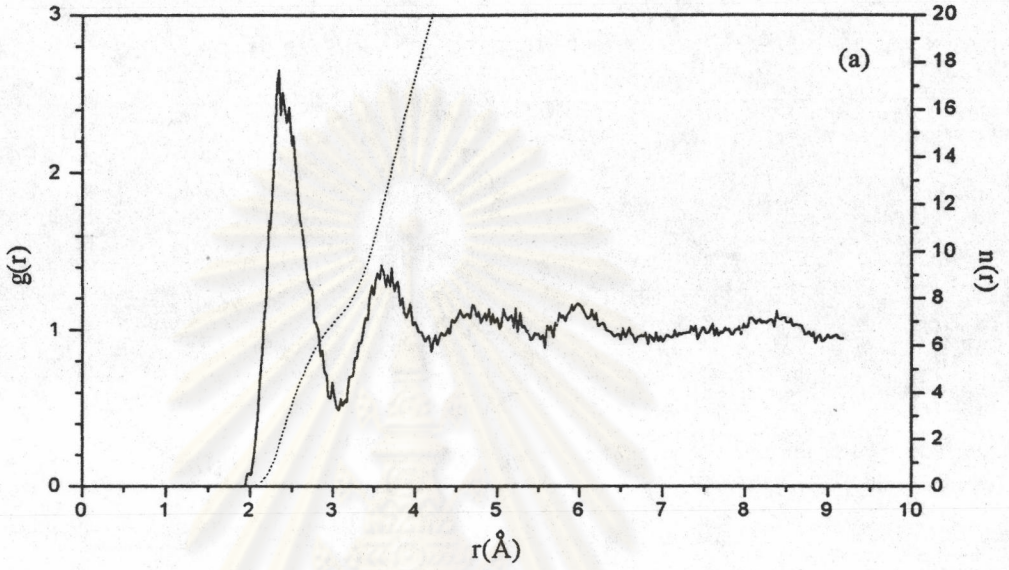

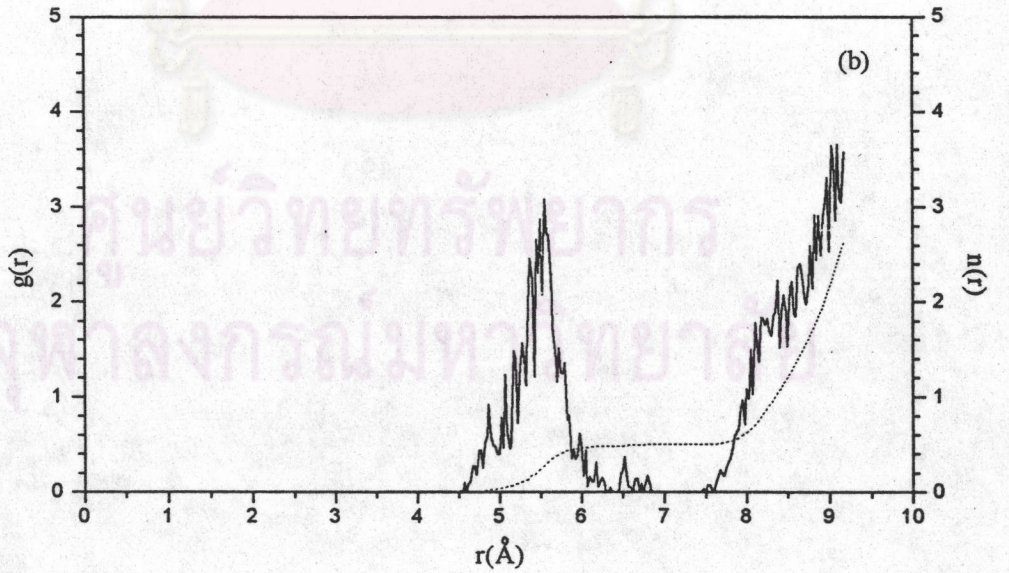

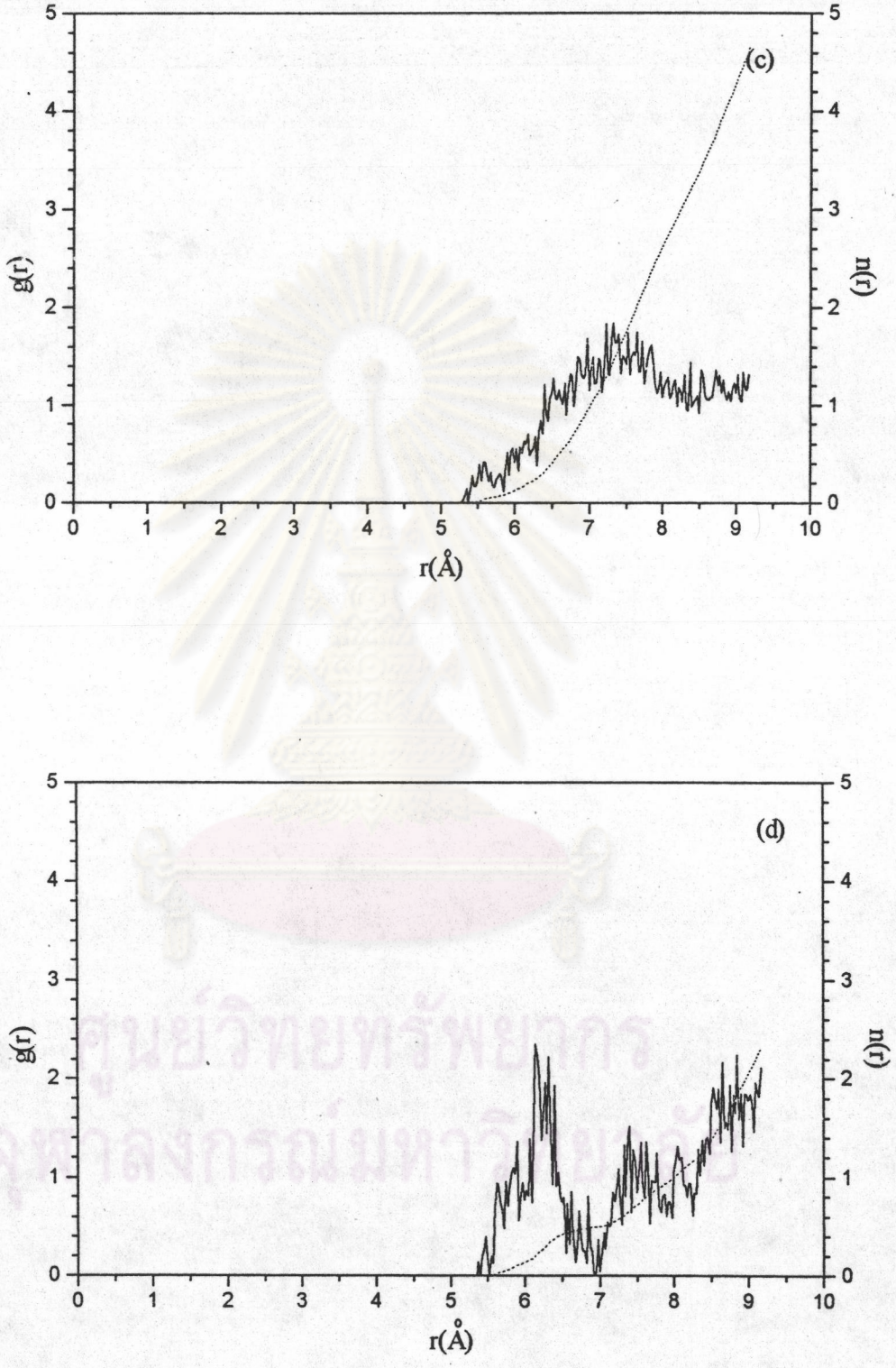

Figure 5.11 Radial distribution functions and running integration numbers for Cl^- in 4.5% by weight NH_2OH ; (a) $Cl\text{-}H_{(w)}$, (b) $Cl\text{-}H_{O(h)}$, (c) $Cl\text{-}H_{N(h)}$, (d) $Cl\text{-}CoM_{(h)}$.

Table 5.5 Characteristic values of radial distribution functions within the first coordination sphere of Cl^- with 4.5% by weight NH_2OH, r_{max} and r_{min} denote the first maximum and minimum of the RDF, and n is the integration up to r_{min}.

RDF	r_{max}	r_{min}	n
$Cl\text{-}CoM_{(w)}$	3.275	3.950	8.0
$Cl\text{-}H_{(w)}$	2.475	3.125	8.0
$Cl\text{-}H_{O(h)}$	-	-	-
$Cl\text{-}H_{N(h)}$	-	-	-
$Cl\text{-}CoM_{(h)}$	-	-	-

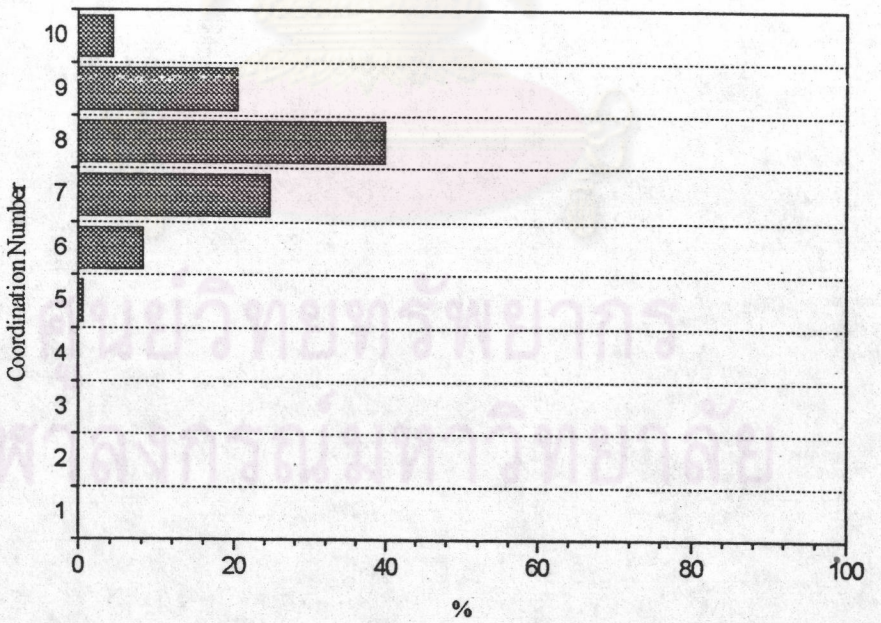

Figure 5.12 Coordination number distribution for $Cl\text{-}CoM_{(w)}$ in 4.5% by weight NH_2OH.

5.6) 25% weight NH_2OH

25% NH_2OH molecules in the solvent, RDFs show in Figure 5.13 and Table 5.6, changed the situation quite drastically. The average solvate species $[Cl(H_2O)_7(NH_2OH)_{4.5}]^-$ results actually from a mixture of species with mostly 6-8 water and either 4 or 5 hydroxylamine ligands. 4 of the H_2O ligands are connected to Cl^- by H-bonds, 3 of the NH_2OH molecules bind to it via NH hydrogen. The fourth NH_2OH ligand can be accommodated through a true OH.... Cl H-bond. The fifth one, if present, is also trying to establish this bond but remains at a more distant, less ideal location recognized form a shoulder at 2.7 Å of the first peak in the $Cl\text{-}H_{O(h)}$ RDF (Figure 5.13 b). The average total coordination number has increased to more than 11, and the transition to bulk allows still to recognize a rather extended second shell around 5-7 Å containing 20 water and 8 NH_2OH molecules.

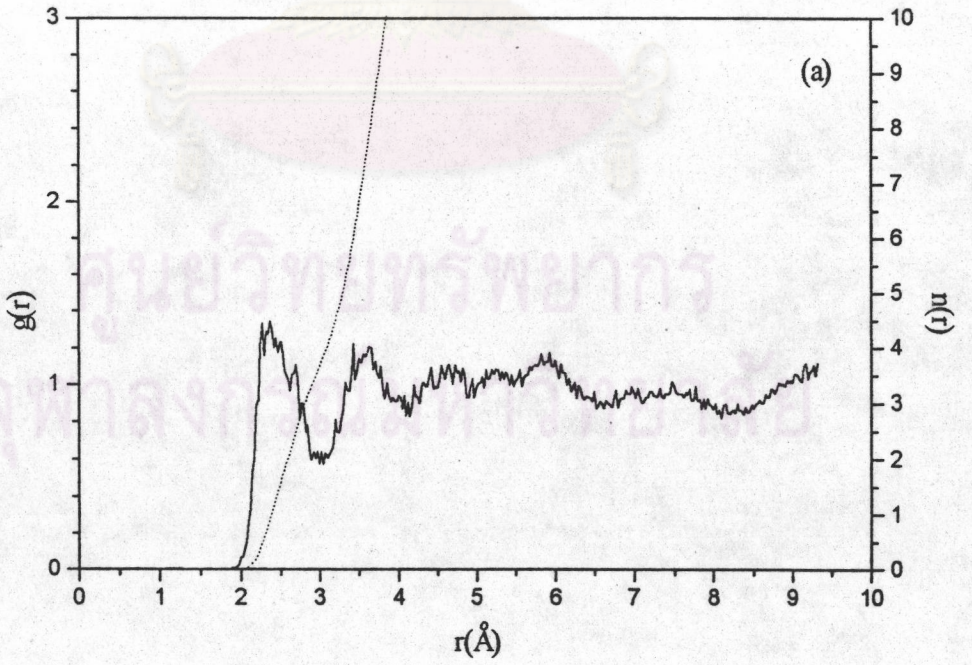

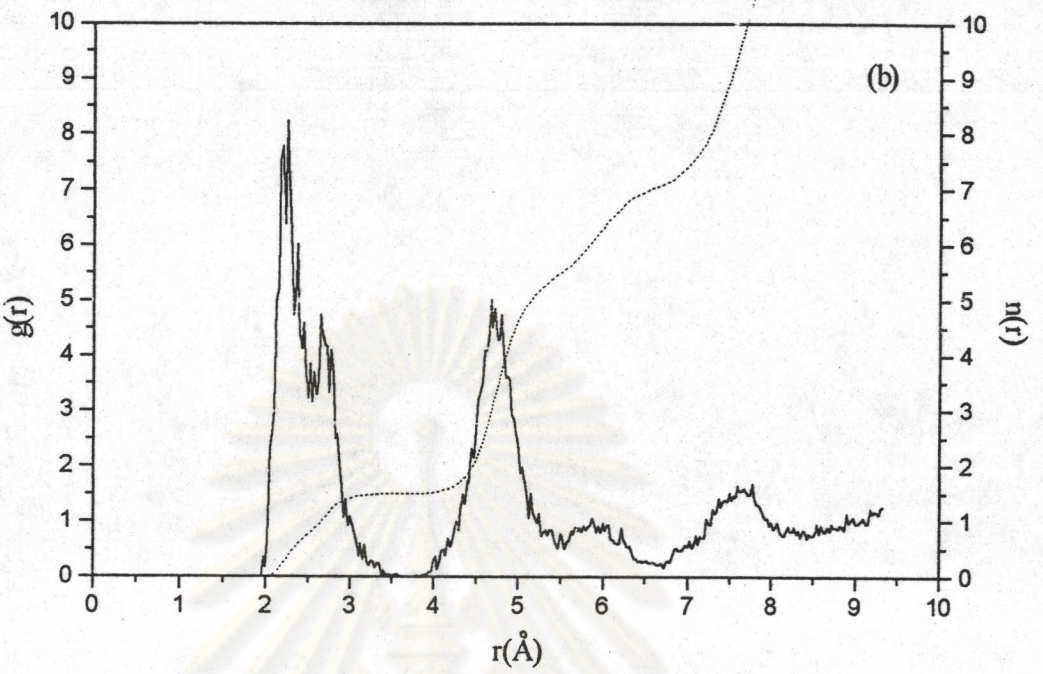

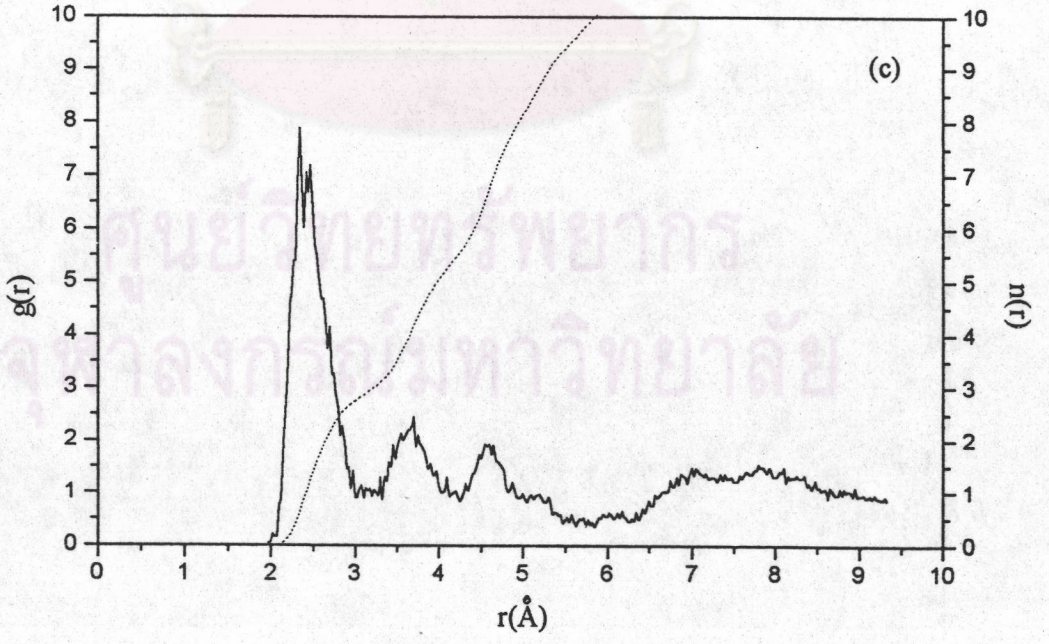

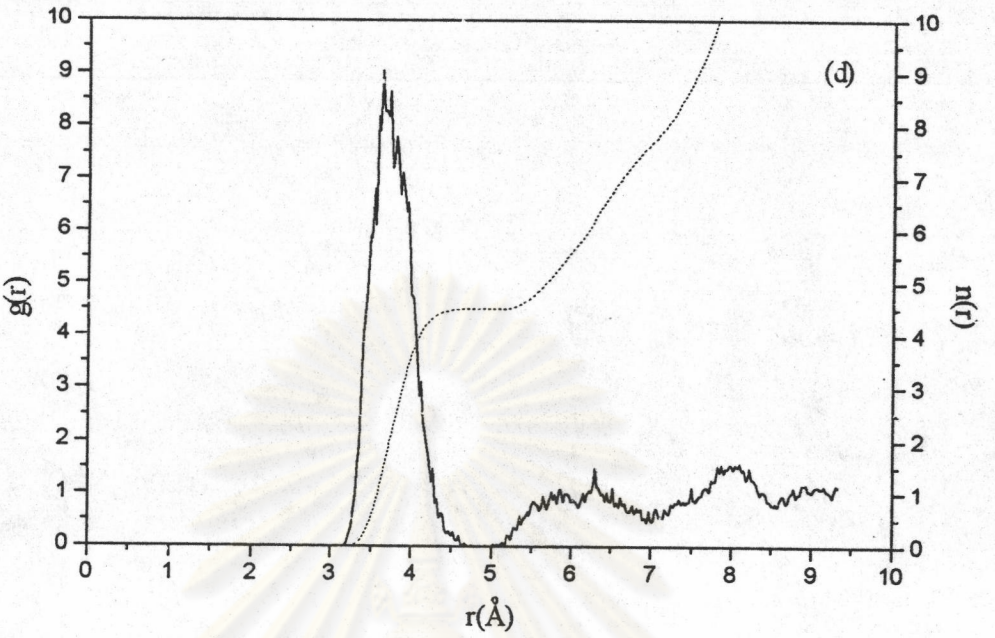

Figure 5.13 Radial distribution functions and running integration numbers for Cl^- in 25% by weight NH_2OH ; (a) $Cl\text{-}H_{(w)}$, (b) $Cl\text{-}H_{O(h)}$, (c) $Cl\text{-}H_{N(h)}$, (d) $Cl\text{-}CoM_{(h)}$.

Table 5.6 Characteristic values of radial distribution functions within the first coordination sphere of Cl^- with 25% by weight NH_2OH, r_{max} and r_{min} denote the first maximum and minimum of the RDF, and n is the integration up to r_{min}.

RDF	r_{max}	r_{min}	n
$Cl\text{-}CoM_{(w)}$	3.300	4.300	7.0
$Cl\text{-}H_{(w)}$	2.375	3.050	4.0
$Cl\text{-}H_{O(h)}$	2.250	3.375	1.5
$Cl\text{-}H_{N(h)}$	2.350	3.325	3.0
$Cl\text{-}CoM_{(h)}$	3.625	4.725	4.5

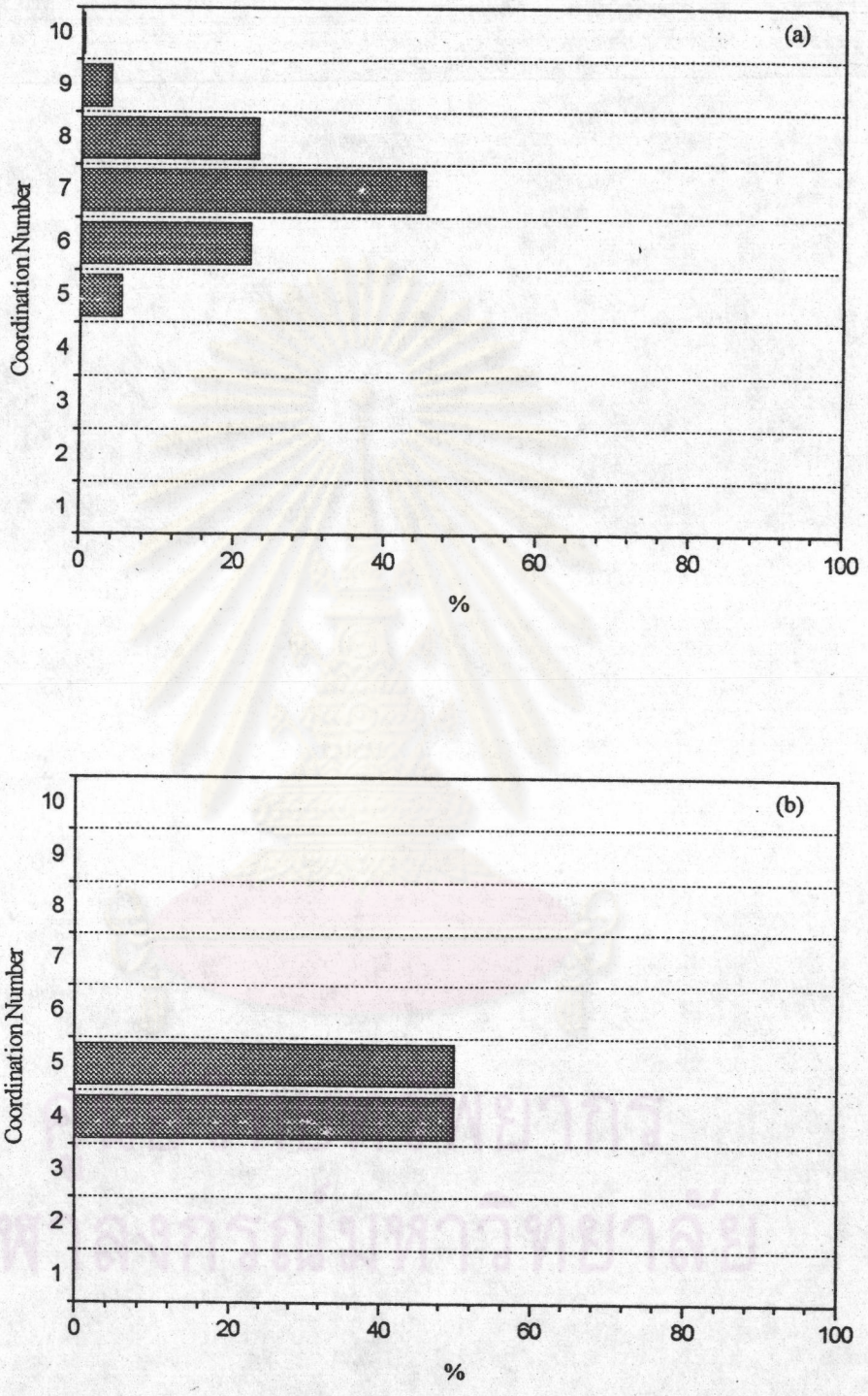

Figure 5.14 Coordination number distribution for (a) Cl-$CoM_{(w)}$ and (b) Cl-$CoM_{(h)}$ in 25% by weight NH_2OH.

5.7) 50% weight NH_2OH

Addition of further hydroxylamine shows that the total coordination number can change easily, according to the mixture's composition. At 50% hydroxylamine content, (Figure 5.15 and Table 5.7), water molecules are ejected from the first solvation layer, but not many of them are replaced by incoming NH_2OH ligands. The average species composition is $[Cl(H_2O)_4(NH_2OH)_4]^-$, corresponding to the statistical average. Analysis of all sampled configuration reveals that this average composition stems from a wide variety, however, where only 53% of the species contain 4 water ligands (Figure 5.16 a); water coordination numbers of 2 and 6 account for about 3% each. and 3 and 5 are present in 17% and 24%, respectively. The contributions of NH_2OH to the solvate composition are mainly 5 (44%), 3 (27%) and 2 (22%) ligands (Figure 5.16 b), whereas the number of 4 ligands, corresponding to the average, is actually found in only 5% of the species. The RDFs show that water molecules in the first shell remain H-bond, and that 1 of the hydroxylamine ligands forms a Cl...HO bond, 2 of them a Cl...HN bond. Other NH_2OH ligands, if present, are associated rather by electrostatic arrangement, not through H-bonds (Figure 5.15 b and c).

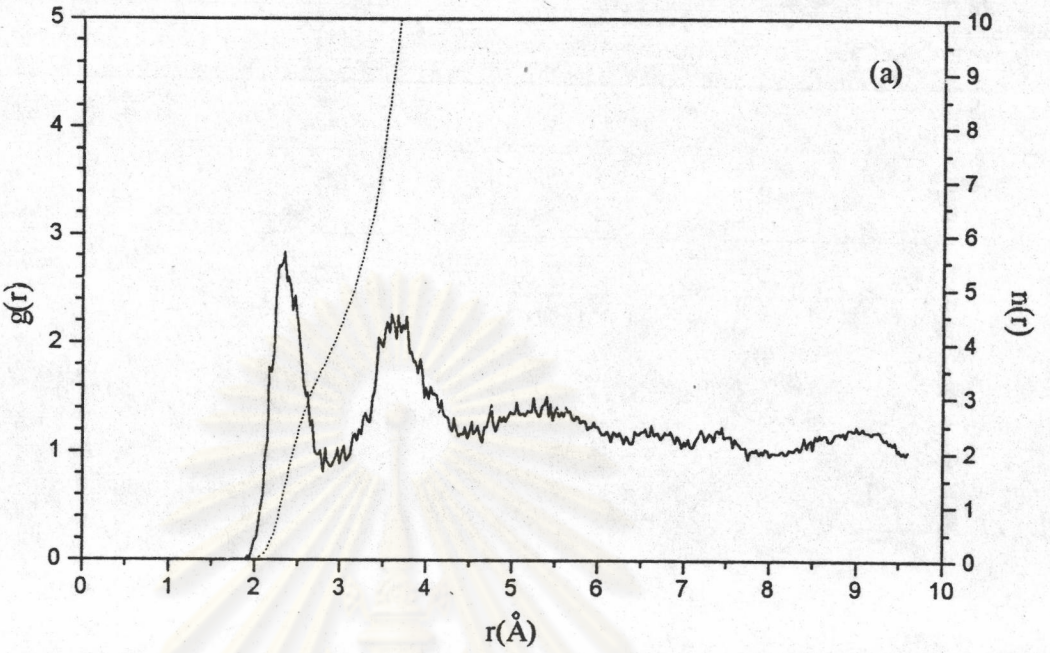
(a)
g(r)
n(r)
r(Å)
0
1
2
3
4
5
6
7
8
9
10

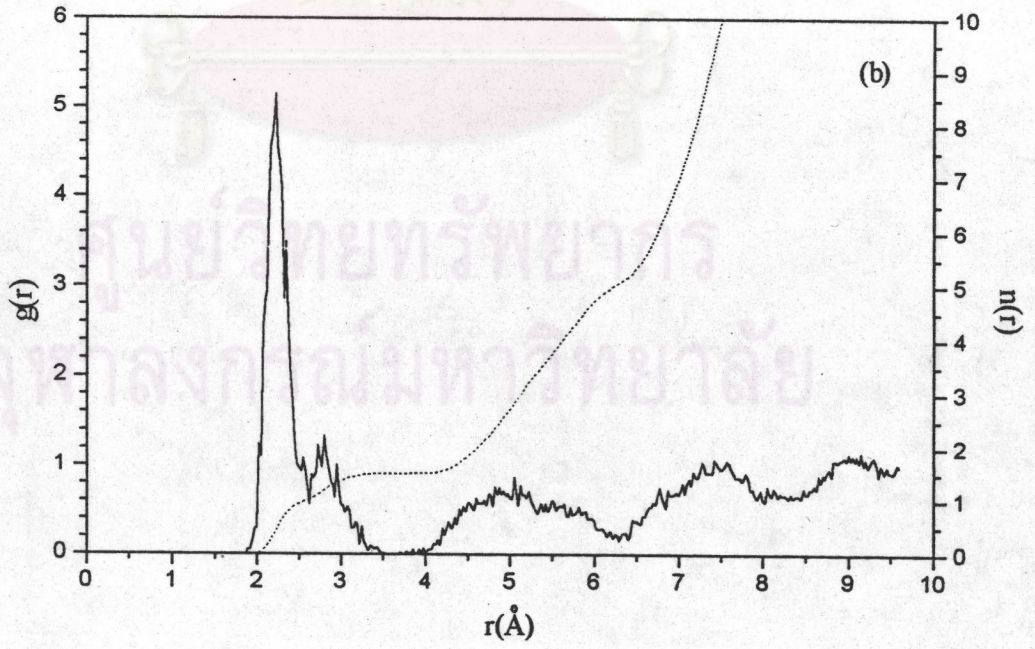
(b)
g(r)
n(r)
r(Å)
0
1
2
3
4
5
6
7
8
9
10

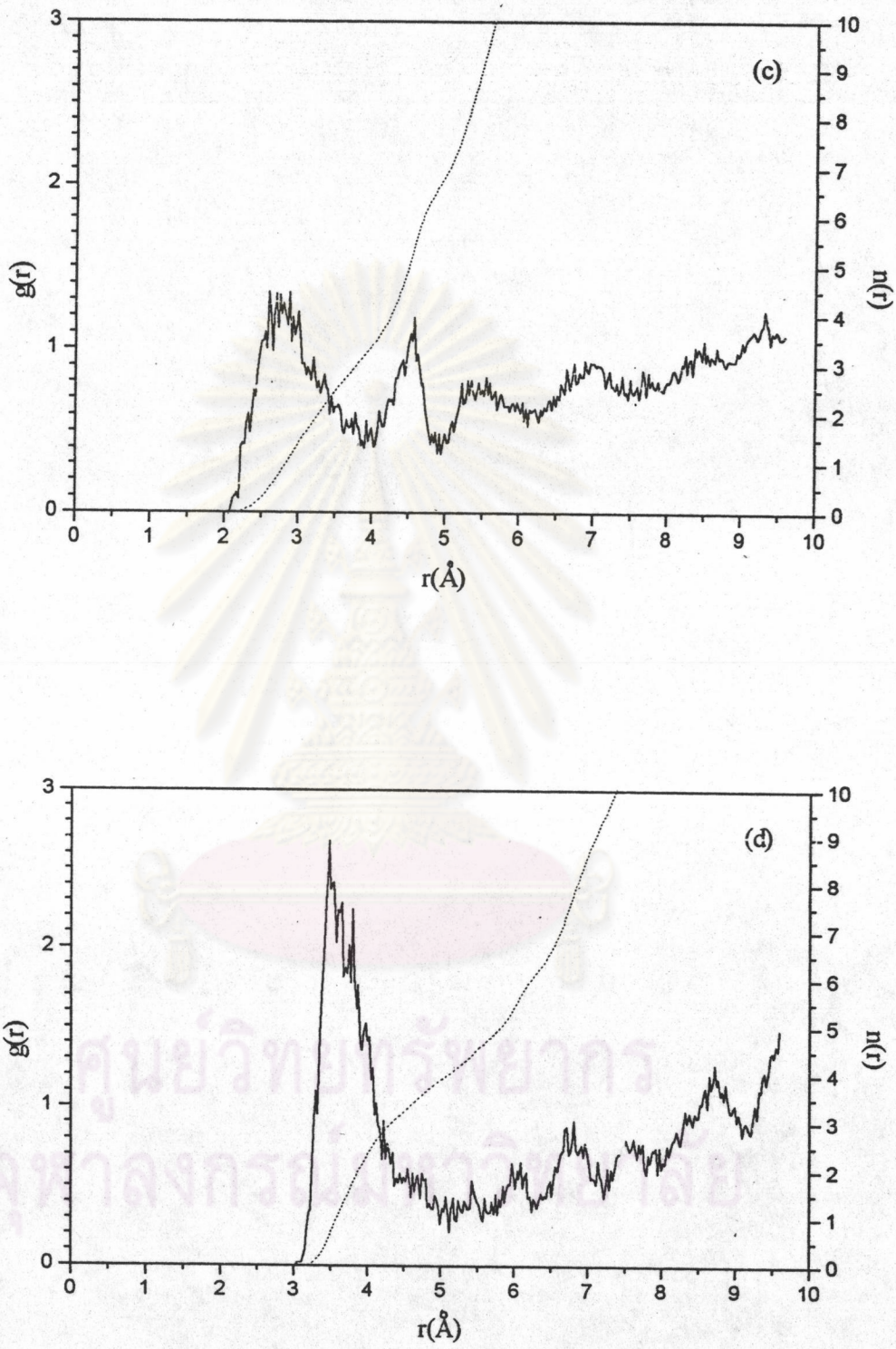

Figure 5.15 Radial distribution functions and running integration numbers for Cl^- in 50% by weight NH_2OH ; (a) $Cl\text{-}H_{(w)}$, (b) $Cl\text{-}H_{O(h)}$, (c) $Cl\text{-}H_{N(h)}$, (d) $Cl\text{-}CoM_{(h)}$.

Table 5.7 Characteristic values of radial distribution functions within the first coordination sphere of Cl^- with 50% by weight NH_2OH, r_{max} and r_{min} denote the first maximum and minimum of the RDF, and n is the integration up to r_{min}.

RDF	r_{max}	r_{min}	n
$Cl\text{-}CoM_{(w)}$	3.200	3.625	4.0
$Cl\text{-}H_{(w)}$	2.350	2.800	4.0
$Cl\text{-}H_{O(h)}$	2.225	3.475	1.5
$Cl\text{-}H_{N(h)}$	2.875	3.900	3.2
$Cl\text{-}CoM_{(h)}$	3.475	5.075	4.0

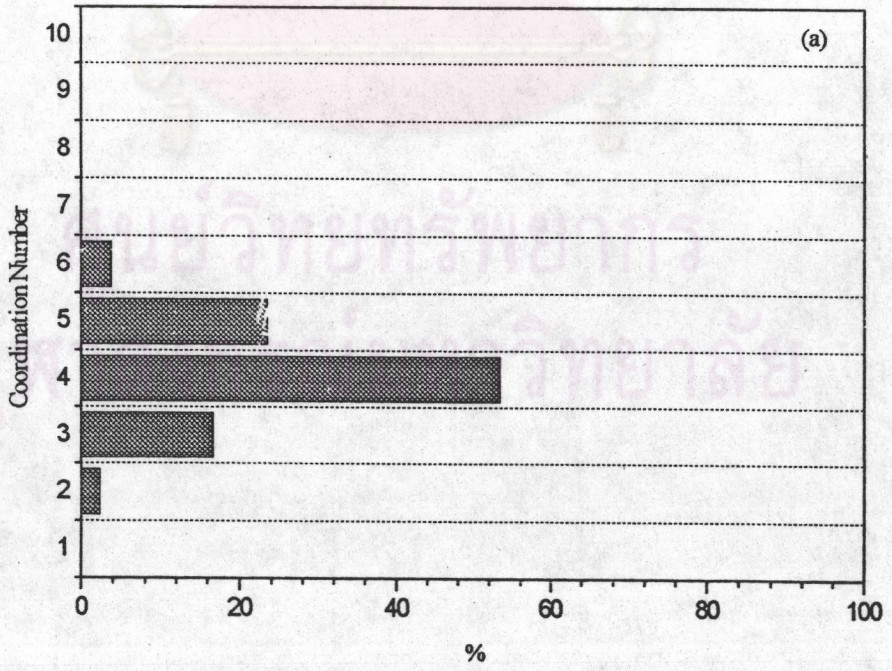

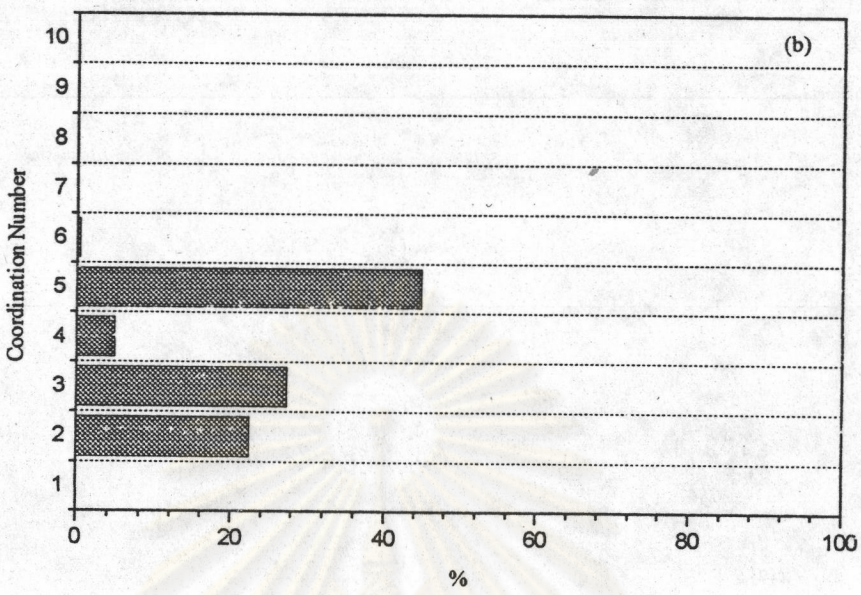

Figure 5.16 Coordination number distribution for (a) Cl-$CoM_{(w)}$ and (b) Cl-$CoM_{(h)}$ in 50% by weight NH_2OH.

5.8) 75% weight NH_2OH

In the 75% NH_2OH mixture (Figure 5.17 and Table 5.8), the solvation shell expands again. The number of water molecules is even slightly higher, than in the 50% solution, and the number of associated hydroxylamine ligand increases considerably, leading to and average composition $[Cl(H_2O)_{4.5}(NH_2OH)_8]^-$, which actually means the incorporation of 4-5 additional (water) ligands into the solvate structure found for pure hydroxylamine, $[Cl(NH_2OH)_8]^-$. The RDFs reveal, however, that only 1 of these water ligands is coordinated via a H bond (Figure 5.17 a), the others are found at larger distances, whereas 3 of the NH_2OH ligands bind to Cl^- through H of OH and 4 to 5 through H of the NH_2 group (Figure 5.17 b and c). In contrast to the average composition, this binding situation rather reflects a preference for NH_2OH as ligand. Water just seems to fill some spaces between the bulkier hydroxylamine ligands. In 85%

of the actual configurations the number of NH_2OH ligands is 8, 9 accounts for 11%, 7 for the rest (Figure 5.18 b). Either 4 or 5 water molecules are present in the first shell, other coordination numbers are only scarcely found (<0.5%) (Figure 5.18 a).

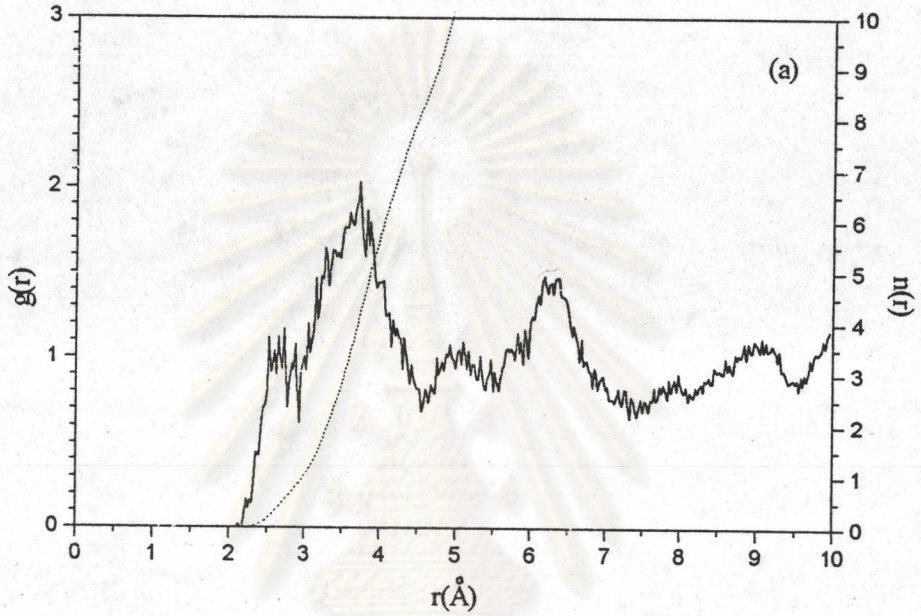

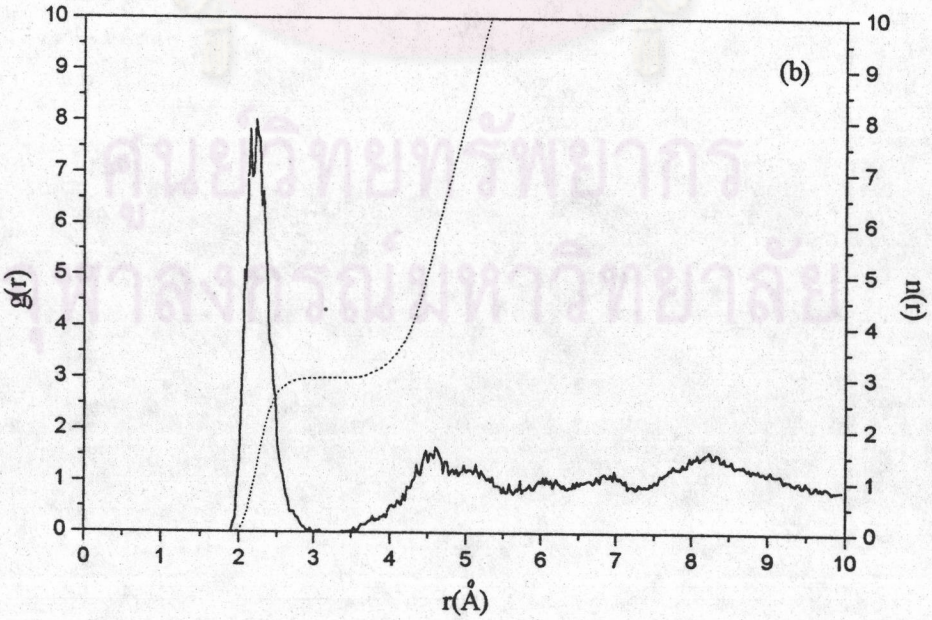

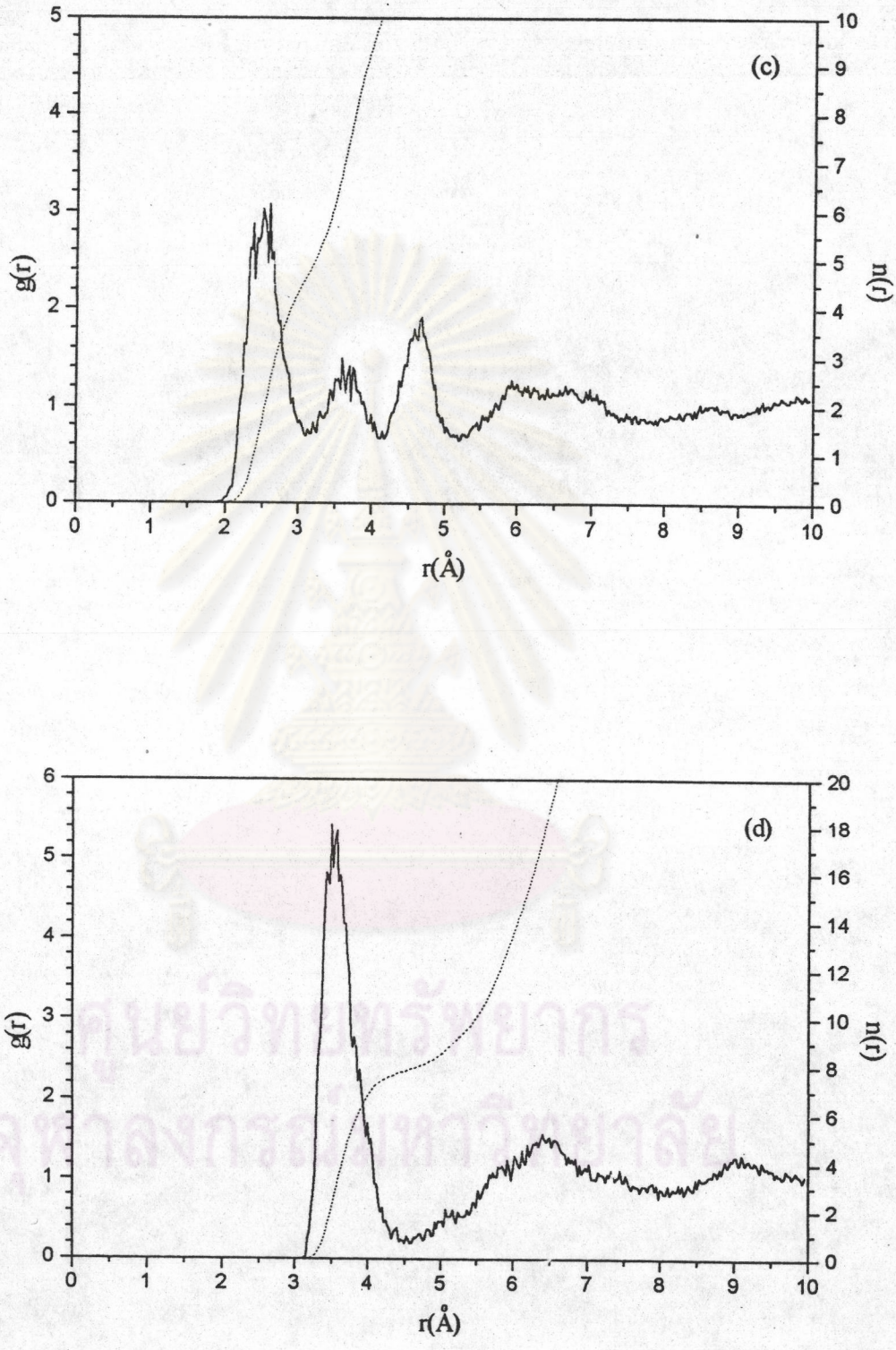

Figure 5.17 Radial distribution functions and running integration numbers for Cl^- in 75% by weight NH_2OH ; (a) $Cl\text{-}H_{(w)}$, (b) $Cl\text{-}H_{O(h)}$, (c) $Cl\text{-}H_{N(h)}$, (d) $Cl\text{-}CoM_{(h)}$.

Table 5.8 Characteristic values of radial distribution functions within the first coordination sphere of Cl^- with 75% by weight NH_2OH, r_{max} and r_{min} denote the first maximum and minimum of the RDF, and n is the integration up to r_{min}.

RDF	r_{max}	r_{min}	n
$Cl\text{-}CoM_{(w)}$	3.975	4.950	4.5
$Cl\text{-}H_{(w)}$	3.725	4.550	8.0
$Cl\text{-}H_{O(h)}$	2.225	2.975	3.0
$Cl\text{-}H_{N(h)}$	2.600	3.175	5.0
$Cl\text{-}CoM_{(h)}$	3.500	4.600	8.0

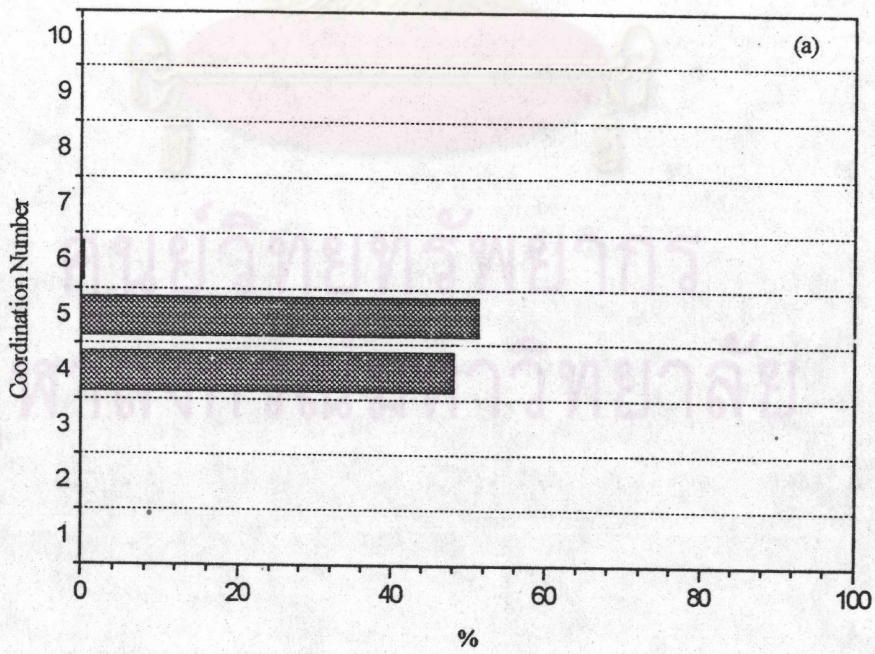

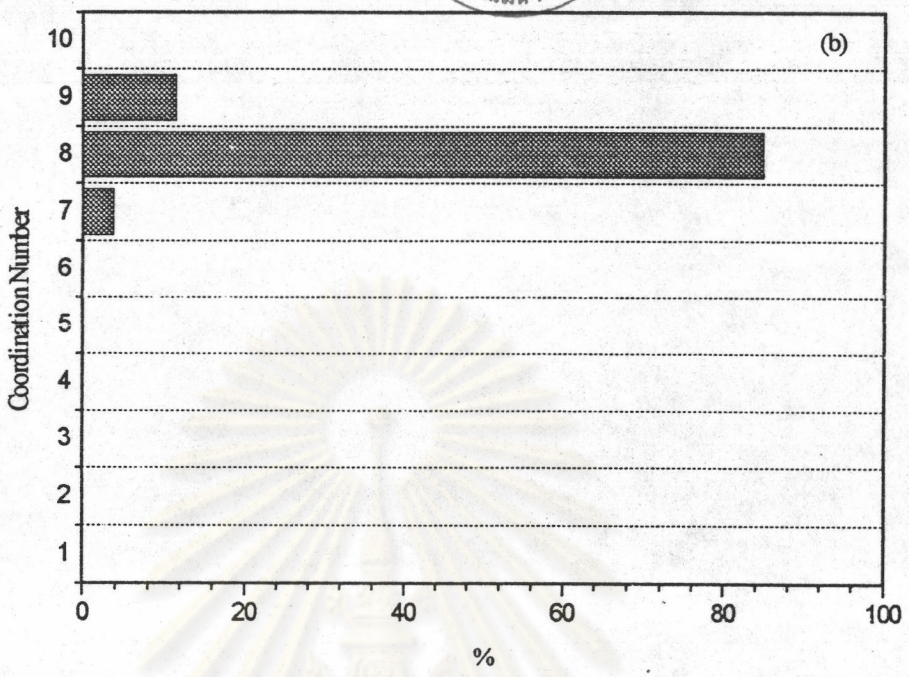

Figure 5.18 Coordination number distribution for (a) Cl-$CoM_{(w)}$ and (b) Cl-$CoM_{(h)}$ in 75% by weight NH_2OH.

A review of all Cl^- related results leads to the conclusion that the composition and structure of the anion's solvation shell is quite sensitive to the solvent's composition and determined mainly by the possibility of forming suitable hydrogen bonds. In the case of hydroxylamine, OH...Cl bonds are stronger and thus the favoured coordination site, but the availability of 2 hydrogens at nitrogen and spatial conditions make this type of coordination equally important. An important difference to cation solvation is the larger size of the first shell, allowing a wider variety of species composition and the association of some molecules in electrostatically determined locations still within that shell.

Synopsis of Solvation Phenomena

The structure data for solvated species formed in the mixed solvent have indicated that - besides the preference for one of the ligands - spatial conditions and compromises between "ideal" binding positions and the ability to accommodate the preferred number of ligands determine the species formation. According to these structural data, a mixture containing between 25% and 50% hydroxylamine seems to offer good conditions in this sense. The wide variety of solvate species present in mixtures of varying NH_2OH content also can be taken as good evidence that exchange processes in the first solvation shell of both cation and anion are easily achieved. This variety also hints at the fact that experimentally determined solvation numbers, besides the difficulty to separate cation and anion contributions, can be misleading in the interpretation of the actual composition of solvates: leading to averaged values they may give a picture strongly deviating from the actual realization of species in solution. At the same time, this points out the importance of a coordination number distribution analysis in addition to the radial distribution functions evaluation.

In order to investigate, which solvent mixture has the best solvating properties for Li^+ and Cl^- ions, a look at the average ion-solvent interaction energies is helpful. The concentration dependent changes of these energies have thus been visualized in Figure 5.19 a and b, together with the changes in the average coordination numbers for both solvents (Figure 5.19 c and d).

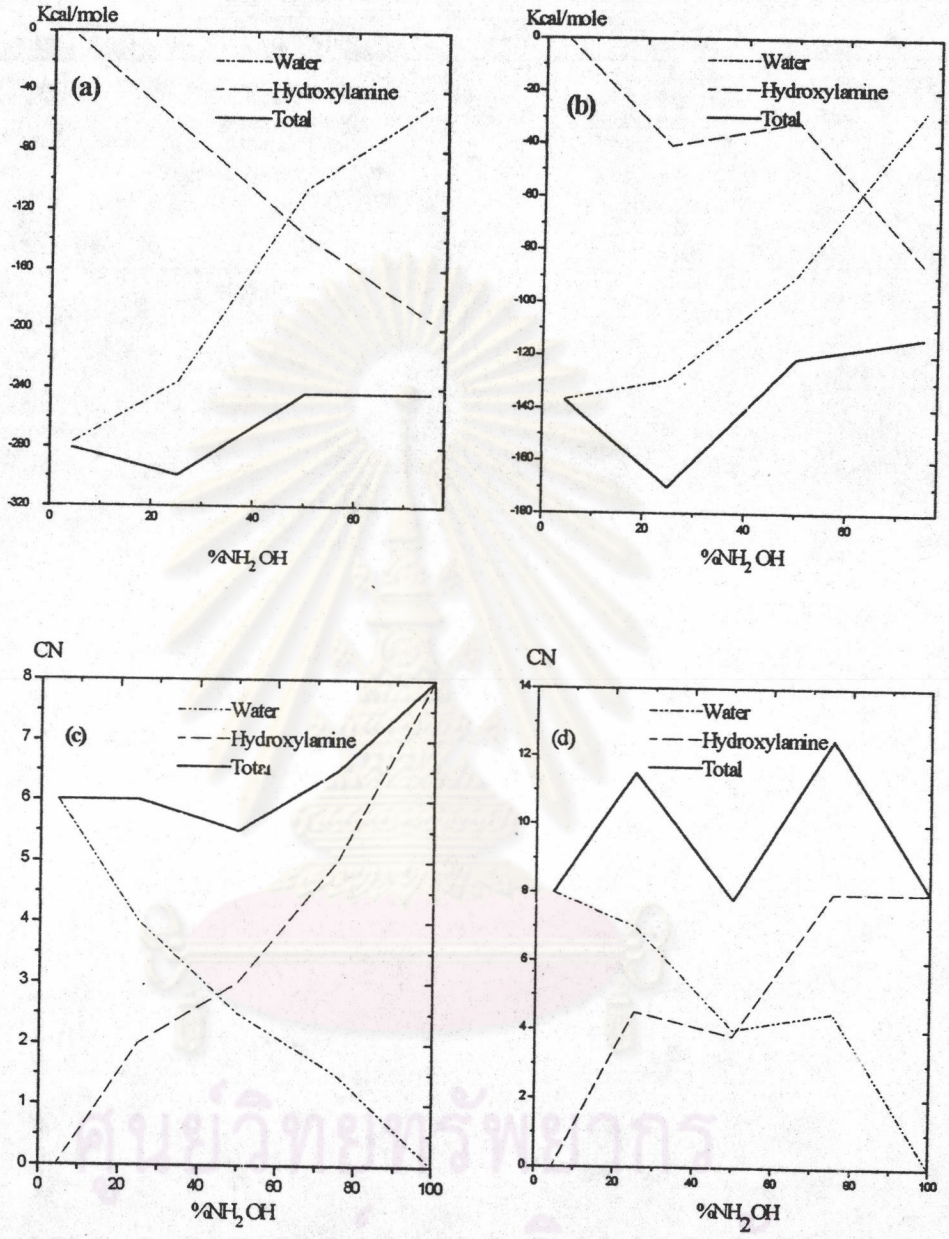

Figure 5.19 Averaged ion-solvent interaction energies for (a) Li^+ and (b) Cl^- and first solvation shell composition for (c) Li^+ and (d) Cl^- in H_2O/NH_2OH mixtures

The graphs for Li^+ ion display a rather continuous change in the composition of the first solvation shell indicating a 1:1 composition at 45% NH_2OH content, where also the energy graphs for interaction with water and hydroxylamine cross. For the total cation solvation energy, the minimum is found when 25% of the solvent consist of NH_2OH, indicating that this mixture provides the energetically best solvating capability, despite of the less ideal structural arrangements of the microspecies formed under this condition.

For the anion, the total coordination number for the first shell fluctuates between 8 and 12.5, reflecting the considerable structural rearrangements induced by the introduction of NH_2OH into the solvent. The graphs for the contribution of both solvents meet at 50%, where 4 ligands of each type are bound to Cl^- (but only in average, as shown in the previous discussion). The interaction energy graphs reveal that the energetically most favourable situation occurs, as in the case of Li^+, with 25% NH_2OH content, the minimum being even more pronounced in the anion's case.

For both cation and anion of LiCl, a 25% aqueous solution of NH_2OH therefore offers the highest solvating power among all mixtures investigated here. It will be of considerable interest to see, which conditions are optimal in the case of other salts, and work pertaining to this question is in progress (32).

CONCLUSIONS

The simulation results presented here give good evidence that statistical thermodynamics simulations of multicomponent electrolyte solutions are a powerful tool to deal with questions related to the microscopic structure of even more complex chemical systems. Preferential solvation phenomena are well accessible and the solvating power of solvent mixtures can be evaluated as well. Simulation techniques can be regarded thus not only as supporting tool for the interpretation of experimental investigations, but - due to their ability of evaluating separately all microspecies in solution - as a practicable way to surpass inherent limitations of experimental methods. Increased availability of intermolecular potential functions will widen this theoretical-chemical approach to solution chemistry to a considerable extent, especially in connection with the continuously decreasing costs of computational power needed for simulations of Monte Carlo and molecular dynamics types.